

# Emergence of criticality in living systems through adaptation and evolution: Practice Makes Critical

Jorge Hidalgo <sup>1†</sup>, Jacopo Grilli, <sup>2†</sup>, Samir Suweis <sup>2</sup>,  
Miguel A. Muñoz <sup>1</sup>, Jayanth R. Banavar <sup>3</sup>, Amos Maritan <sup>2\*</sup>

<sup>1</sup> Departamento de Electromagnetismo y Física de la Materia and  
Instituto Carlos I de Física Teórica y Computacional.

Universidad de Granada. E-18071, Granada, Spain

<sup>2</sup> Dipartimento di Fisica ‘G. Galilei’ & CNISM, INFN.

Università di Padova, Via Marzolo 8, 35131 Padova, Italy

<sup>3</sup> Department of Physics, University of Maryland, College Park, MD 20742, USA

† These authors contributed equally to this work

\* To whom correspondence should be addressed: amos.maritan@pd.infn.it

## Abstract

Empirical evidence has proliferated that living systems might operate at the vicinity of critical points<sup>1</sup> with examples ranging from spontaneous brain activity<sup>2-6</sup> to flock dynamics.<sup>7</sup> Such systems need to cope with and respond to a complex ever-changing environment through the construction of useful internal maps of the world. Here we employ tools from statistical mechanics and information theory to prove that systems poised at criticality are much more efficient in ensuring that their internal maps are good proxies of reality. Analytical and computational evolutionary models vividly illustrate that a community of such systems dynamically self-tunes toward a critical state either as the complexity of the environment increases or even upon attempting to map with fidelity the other agents in the community. Our approach constitutes a general explanation for the emergence of critical-like behavior in complex adaptive systems.

It is believed that living systems (or parts, aspects, or groups of them) benefit from having attributes akin to criticality such as large dynamical repertoire and extremal sensitivity to external changes,<sup>4,8-14</sup> and that complex computations can only be performed by machines operating at criticality.<sup>15</sup> Unlike models of self-organized criticality,<sup>16</sup> our goal here is to uncover general adaptive or evolutionary mechanisms –specific of living systems– through which such self-tuning to criticality might occur, thereby conferring them with functional advantages.

An invaluable hint for understanding how and why the apparently ubiquitous self-tuning to criticality occurs in living systems is provided by the immortal words of Borges describing the strong need for limited but informative representations of reality<sup>17</sup> “In that Empire, the Art of Cartography attained such Perfection that the map of a single Province occupied the entirety of a City, and the map of the Empire, the entirety of a Province. In time, those Unconscionable Maps no longer satisfied, and the Cartographers Guilds struck a Map of the Empire whose size was that of the Empire, and which coincided point for point with it. The following generations . . . saw that that vast Map was Useless . . .” The successful constructions of internal representations, which extract, summarize, and integrate relevant information,<sup>18</sup> provides a crucial competitive advantage, which can eventually make the difference between survival and extinction.<sup>19</sup> It has been suggested<sup>20,21</sup> that the role of early sensory neurons is to remove statistical redundancy in the sensory input and that computations in the brain serve to construct efficient representations of in-coming sensory data; variants of this “efficient coding hypothesis” have been thoroughly studied (e.g.<sup>22</sup>), and concrete evidence has been found of the brain building representations of the sensory world that are efficient in the sense of information theory.<sup>23</sup> Similar principles are relevant for artificial intelligence and evolutionary robotics.<sup>18,24,25</sup>

These general ideas can be exploited to construct a quantitative framework, which clearly demonstrates that self-tuning to criticality is a strategy adopted by living systems to effectively represent the external world. The critical point reached in this way represents a borderline between a disordered phase in which perturbations and noise propagate unboundedly and an ordered phase whereas changes are rapidly erased –hindering plasticity– thereby providing an excellent compromise between flexibility and accuracy.

Consider a stimulus from a given environmental *source* processed through the sensory perception system. To be concrete, let us, without loss of generality, represent the stimulus by a string of  $N$  (binary) variables,  $\mathbf{s} = (s_1, s_2, \dots, s_N)$ . A specific environmental source is modeled by the probability distribution  $P_{src}$ , with which it produces each of the  $2^N$  possible signals; for concreteness, this distribution is assumed to depend on a set of parameters (that we call  $\boldsymbol{\alpha} = (\alpha_1, \alpha_2, \dots)$ ). Allowing these parameters to vary, different sources can be modelled.

We turn now to an individual (cognitive) system or agent, which seeks to represent, with the largest possible fidelity, the essential aspects of the stimuli emanating from a given environmental source but (in the spirit of Borges paradox) employing a much smaller number of parameters (that we denote by  $\boldsymbol{\beta} = (\beta_1, \beta_2, \dots)$ ). This is accomplished through an internal representation or map, encapsulated in a second probability distribution function,  $P_{map}$ , that aims to capture the essential features of  $P_{src}$ . Different values of these parameters allow for different realizations of the internal maps. Here we show that –under very broad conditions– there exists an optimal set of map parameters, which lies in the vicinity of a critical point and ensures the best possible representation of the environmental source(s).

Information theory provides us with a robust measure of the “closeness” between the source probability distribution and its map through the Kullback-Leibler (KL) divergence,<sup>26</sup>  $D(\boldsymbol{\alpha}|\boldsymbol{\beta})$ , which quantifies the information loss when the map is used to approximate the source (see Methods). The KL divergence is never negative and vanishes if and only if the two involved probability distributions are identical, as would occur for a Borges map. Minimizing the KL divergence with respect to the map (limited) parameters generates the optimal, though imperfect, mapping of any given environmental source (see Fig. 1A). However, in an ever-changing world, the requirement for an individual is not to just to reproduce a single source with utmost fidelity but rather to successfully map a group of highly diverse sources (see Fig. 1B). A special case of this, would comprise a group of similar individuals which together strive to establish some kind of common understanding (see Fig. 1C). In any of these complex situations, an individual has a better *fitness*, when a characteristic measure, e.g. the mean, of the KL divergences from the set

of diverse sources is small.

We have developed diverse computational evolutionary models inspired by the genetic algorithm.<sup>27,28</sup> In all of these, a community of  $M$  individuals –each one characterized by its own set of internal parameters  $\beta$ – evolves in time through the processes of death, birth, and mutation (see Methods). Individuals with larger fitness, i.e. with a smaller mean KL divergence from the rest of sources, have a larger probability to produce an offspring which –apart from small random mutations– inherits its parameters from its ancestor, while agents with low fitness are more likely to die and be removed from the community. We have studied two types of models (evolutionary and co-evolutionary) which differ in the ways in which the environmental sources are treated.

In the first *evolutionary* model (see Fig. 2),  $M$  systems are exposed to an environment of  $S$  independent heterogeneous environmental sources, each one with different  $P_{src}$  (and thus with diverse  $\alpha$ 's). The set of  $S$  sources is randomly extracted from a broadly distributed pool  $\rho_{src}(\alpha)$ . The fitness of an individual with parameters  $\beta$  is a decreasing function of the average KL divergence from external stimuli

$$d(\beta|\rho_{src}) := \int d\alpha \rho_{src}(\alpha) D(\alpha|\beta) . \quad (1)$$

Upon iterating the genetic algorithm, the map parameters  $\beta$  evolve, leading to a steady-state stable distribution. Computer simulations show that in the case of very specific environments, occurring when all sources in the pool are similar, the optimal  $\beta$  strongly depends on the sources, resulting in a detail-specific mapping. Quite remarkably, if the external world is sufficiently variable/complex the optimal map is detail-independent and it becomes sharply peaked around the critical point (Supplementary Video 1 illustrates the evolution of agents concentrating around criticality).

In the second *co-evolutionary* model (see Fig. 3), the environment is modeled in a dynamical way so that no *a priori* choice is made for the pool of sources, but instead, they emerge from the systems' own evolution in a self-consistent manner. In particular, the environment perceived by each individual consists of the other  $M - 1$  systems, which it aims at “understanding” and mapping. In the simplest computational implementation of this idea (see Methods), a pair of individual systems is randomly selected at each time

step. Each of the individuals provides the environmental source for the other. Because the KL divergence is not symmetric respect to the interchange of the probability distributions (see Methods), one of the two systems has a larger fitness and hence a greater probability of generating progeny, while the less fit system is more likely to die. This corresponds to an effective fitness of agent  $i$  which is a decreasing function of the average KL divergence from the rest of individuals

$$d(\{\beta_j\}_{j \neq i} | \beta_i) := \frac{1}{M-1} \sum_{j \neq i} D(\beta_j | \beta_i) \quad (2)$$

In this case, as illustrated in Fig. 3 (and in Supplementary Videos 2 and 3), the co-evolution of systems and sources leads to a very robust evolutionarily-stable steady-state distribution which is peaked around criticality (see SI).

These computational results are supported by analytical calculations (see Methods and detailed calculations in the SI) showing that in the case of highly diverse sources, the probability of having an optimal mapping characterized by some parameter set is proportional to its *generalized susceptibility* (or, equivalently, to the *Fisher information*<sup>26</sup>) which is well-known to become very large in the vicinity of critical points and to diverge in the limit of infinitely many codification bits,  $N$ ,<sup>8</sup> as would be the case of sensory systems. Different analytical calculations (see SI) illustrate that *a collection of cognitive systems evolves and eventually clusters around the critical state in the presence of broadly different ever-changing environments*. This conclusion can also be understood in the language of statistical mechanics as the internal map at criticality is best able to encode distributions characteristic of both disordered and ordered phases and can accommodate a wide range of stimuli configurations with non-zero weight. Indeed, it has been recently shown that many more distinguishable outputs can be reproduced by models poised at criticality.<sup>29</sup>

The ideas presented here apply most straightforwardly in neuroscience and could contribute to a better understanding of why neural activity seems to be tuned to criticality, but it has much broader implications. For example, in the context of Boolean networks (i.e. minimal models of genetic regulatory networks),<sup>30</sup> criticality was shown to emerge through adaptive information processing. Boolean networks can be trained to produce a desired output from a given input in a noisy environment; however, when tasks of very

different complexity need to be learned simultaneously, networks adapt to a critical state to enhance their performance,<sup>31</sup> which is a very natural result within our framework.

In summary, we propose a framework for understanding systems striving to cope with a complex and heterogeneous external world. To do so successfully, they must first build an efficient, though approximate, “internal representation” or map of the environment and base their response on it. The better the map, the more effective their reactions and the more superior their performance. We have translated these ideas into a general mathematical framework and, by using techniques of statistical physics and information theory, we have been able to show –in a variety of examples– that the best possible trade-off between accuracy and flexibility for “internal maps” of complex environments is obtained by operating at criticality. Instead, if the environment is fixed, homogeneous and predictable –which is not usually the case– agents do not need to become critical. In this sense, the observed criticality in living systems can be understood as resulting from the interplay between their need for producing accurate maps of the world, their need to cope with many widely diverse environmental conditions, and their well-honed ability to react to external changes in an optimal way. Evolution drives cognitive systems to criticality in response to this smart cartography.

## Methods

**Kullback-Leibler divergence** . Given two probability distributions  $P(\mathbf{s})$  and  $Q(\mathbf{s})$  for the set of variables  $\mathbf{s}$ , the Kullback-Leibler (KL) divergence of  $Q(\mathbf{s})$  from  $P(\mathbf{s})$  is defined as

$$D(P(\cdot)|Q(\cdot)) := \sum_{\mathbf{s}} P(\mathbf{s}) \log\left(\frac{P(\mathbf{s})}{Q(\mathbf{s})}\right), \quad (3)$$

and quantifies the loss of information when  $Q(\mathbf{s})$  is used to approximate  $P(\mathbf{s})$ .<sup>26</sup> Indeed, in the large  $T$  limit, the probability  $\mathcal{L}$  that the model  $Q(\mathbf{s})$  generates a sequence of  $T$  observations compatible with  $P(\mathbf{s})$  can be computed as  $\mathcal{L} \sim \exp\left(-T \sum_{\mathbf{s}} D(P(\mathbf{s})|Q(\mathbf{s}))\right)$  up to leading order (see SI). Therefore, maximizing the likelihood of a trial probability distribution function  $Q$  is equivalent to minimizing its KL divergence with respect from the original one,  $P$ .

**Fisher Information and criticality** Let the set of random variables  $\mathbf{s} = \{s_1, \dots, s_N\}$  be distributed as  $P(\mathbf{s}|\boldsymbol{\beta})$  with some dependency on parameters  $\boldsymbol{\beta}$ .  $P(\mathbf{s}|\boldsymbol{\beta})$  can quite generally be written as

$$P(\mathbf{s}|\boldsymbol{\beta}) = \frac{\exp(-H(\mathbf{s}|\boldsymbol{\beta}))}{Z(\boldsymbol{\beta})}, \quad (4)$$

where the factor  $Z(\boldsymbol{\beta})$  is fixed through normalization. The function  $H$  can be written as

$$H(\mathbf{s}|\boldsymbol{\beta}) = \sum_{\mu} \beta_{\mu} \phi^{\mu}(\mathbf{s}), \quad (5)$$

where  $\phi_{\mu}(\mathbf{s})$  are suitable functions (“observables”). With this parametrization, the *Fisher information* or *generalized susceptibility* is the matrix  $\boldsymbol{\chi}$  whose elements are defined as

$$\chi^{\mu\nu}(\boldsymbol{\beta}) := \frac{\partial^2 \log(Z)}{\partial \beta_{\mu} \partial \beta_{\nu}} = \langle \phi^{\mu} \phi^{\nu} \rangle_{\boldsymbol{\beta}} - \langle \phi^{\mu} \rangle_{\boldsymbol{\beta}} \langle \phi^{\nu} \rangle_{\boldsymbol{\beta}}, \quad (6)$$

where the average  $\langle \cdot \rangle_{\boldsymbol{\beta}}$  performed with respect to  $P(\cdot|\boldsymbol{\beta})$ . At least one of the matrix elements diverges in the limit  $N \rightarrow \infty$  if the system exhibits a critical point  $\boldsymbol{\beta} = \boldsymbol{\beta}_c$ .

**Evolutionary model.** A community of agents receiving external stimuli from an outer and heterogeneous environment is modeled as follows. Every specific environmental source corresponds to a probability distribution  $P_{src}(\mathbf{s}|\boldsymbol{\alpha}) \propto \exp(-H_{src}(\mathbf{s}|\boldsymbol{\alpha}))$ , with  $H_{src}(\mathbf{s}|\boldsymbol{\alpha}) = \sum_{\mu}^E \alpha_{\mu} \phi_{src}^{\mu}(\mathbf{s})$ , where the parameters  $\boldsymbol{\alpha}$  are drawn from the distribution  $\rho_{src}(\boldsymbol{\alpha})$ . The  $k$ -th agent in the community constructs an internal representation of

the observed source described by  $P_{map}(\mathbf{s}|\boldsymbol{\beta}^k) \propto \exp(-H_{map}(\mathbf{s}|\boldsymbol{\beta}^k))$  with  $H_{map}(\mathbf{s}|\boldsymbol{\beta}^k) = \sum_{\nu} \beta_{\nu}^k \phi_{map}^{\nu}(\mathbf{s})$ , with parameters  $\boldsymbol{\beta}^k$ . We start with  $M$  individuals each one equipped with some initial parameter set extracted from some arbitrary distribution  $p(\boldsymbol{\beta}, t = 0)$ . At every time step, we generate  $S$  external sources, parameters,  $\{\boldsymbol{\alpha}^u\}_{u=1,\dots,S}$ , from the source-pool  $\rho_{src}(\boldsymbol{\alpha})$ . Then we compute the average KL divergence of every individual's mapping from the external sources

$$d(\{\boldsymbol{\alpha}^u\}|\boldsymbol{\beta}^k) := \frac{1}{S} \sum_{u=1}^S \sum_{\mathbf{s}} P_{src}(\mathbf{s}|\boldsymbol{\alpha}^u) \log \frac{P_{src}(\mathbf{s}|\boldsymbol{\alpha}^u)}{P_{map}(\mathbf{s}|\boldsymbol{\beta}^k)}. \quad (7)$$

The  $k$ -th individual of the community is removed with a probability proportional to its average KL divergence (or any increasing function of it)

$$P_{kill}(k) = \frac{d(\{\boldsymbol{\alpha}^u\}|\boldsymbol{\beta}^k)}{\sum_l d(\{\boldsymbol{\alpha}^u\}|\boldsymbol{\beta}^l)} \quad (8)$$

and it is replaced by an offspring of another individual randomly selected from the rest of the community. The offspring inherits its parameters  $\boldsymbol{\beta}$  from its parent and mutates with a probability  $\nu$ , altering the original parameter set,  $\boldsymbol{\beta} \rightarrow \boldsymbol{\beta} + \boldsymbol{\xi}$ , where  $\boldsymbol{\xi}$  is a multivariate Gaussian random vector, with uncorrelated components, zero mean and variance  $\sigma^2$ . Finally, time is incremented as  $t \rightarrow t + 1/M$ , another set of parameters  $\{\boldsymbol{\alpha}^u\}_{u=1,\dots,S}$  is generated, and the process is iterated. Parameter values are shown in the SI.

**Co-evolutionary model.** Every individual receives stimuli from its surrounding world, which is nothing but the set of the individuals in the community. More specifically: the  $k$ -th agent of the community is described by a probability distribution  $P_{map}(\mathbf{s}|\boldsymbol{\beta}^k) \propto \exp\{-H_{map}(\mathbf{s}|\boldsymbol{\beta}^k)\}$ , depending on parameters  $\boldsymbol{\beta}^k$ . Starting with an ensemble of  $M$  individuals whose coupling parameters are extracted from an arbitrary distribution,  $p(\boldsymbol{\beta}, t = 0)$ , the evolutionary dynamics proceeds as follows: At each time step, two individuals,  $i$  and  $j$ , are randomly selected. Their relative fitnesses  $f_i^{(j)}$  and  $f_j^{(i)}$  are computed as

$$f_i^{(j)} = 1 - \frac{D(\boldsymbol{\beta}^j|\boldsymbol{\beta}^i)}{D(\boldsymbol{\beta}^j|\boldsymbol{\beta}^i) + D(\boldsymbol{\beta}^i|\boldsymbol{\beta}^j)}, \quad (9)$$

and similarly for  $f_j^{(i)}$ . As the KL divergence is not symmetric,  $f_i^{(j)} \neq f_j^{(i)}$  unless  $\boldsymbol{\beta}^i = \boldsymbol{\beta}^j$ , one of the two individuals –selected with probability equal to its relative fitness– creates



an offspring, while the other one is removed from the community. As in the Evolutionary Model, the offspring inherits its parameters from its ancestor (with prob.  $1 - \nu$ ) or mutates with a probability  $\nu$ , modifying its parameters from  $\beta$  to  $\beta \rightarrow \beta + \xi$ , where  $\xi$  is a multivariate Gaussian random vector, with uncorrelated components, zero mean and variance  $\sigma^2$ . Time is updated to  $t \rightarrow t + 1/M$ , another couple of individuals  $i'$  and  $j'$  is picked, and the process is iterated. The SI describes other variants of this model.

**Acknowledgements** A.M. and S.S. acknowledge Cariparo foundation for financial support. M.A.M. and J.H. acknowledge support from J. de Andalucia P09-FQM-4682 and the Spanish MINECO FIS2009-08451. We thank T. Hoang, J. Uriagereka, S. Vassanelli and M. Zamparo for insightful discussions.

## References

- [1] Mora, T. & Bialek, W. Are biological systems poised at criticality? *Journal of Statistical Physics* **144**, 268–302 (2011).
- [2] Beggs, J. & Plenz, D. Neuronal avalanches in neocortical circuits. *The Journal of neuroscience* **23**, 11167–11177 (2003).
- [3] Plenz, D. & Thiagarajan, T. C. The organizing principles of neuronal avalanches: cell assemblies in the cortex? *Trends in neurosciences* **30**, 101–110 (2007).
- [4] Chialvo, D. R. Emergent complex neural dynamics. *Nature Physics* **6**, 744–750 (2010).
- [5] Shriki, O. *et al.* Neuronal avalanches in the resting MEG of the human brain. *The Journal of Neuroscience* **33**, 7079–7090 (2013).
- [6] Haimovici, A., Tagliazucchi, E., Balenzuela, P. & Chialvo, D. R. Brain organization into resting state networks emerges at criticality on a model of the human connectome. *Phys. Rev. Lett* **110**, 178101 (2013).

- [7] Bialek, W. *et al.* Statistical mechanics for natural flocks of birds. *Proceedings of the National Academy of Sciences* **109**, 4786–4791 (2012).
- [8] Stanley, H. E. *Introduction to phase transitions and critical phenomena* (Oxford University Press, 1987).
- [9] Legenstein, R. & Maass, W. Edge of chaos and prediction of computational performance for neural circuit models. *Neural Networks* **20**, 323–334 (2007).
- [10] Pfaff, D. & Banavar, J. R. A theoretical framework for CNS arousal. *Bioessays* **29**, 803–810 (2007).
- [11] Beggs, J. M. The criticality hypothesis: How local cortical networks might optimize information processing. *Phil. Trans. R. Soc. A* **366**, 329–343 (2008).
- [12] Kinouchi, O. & Copelli, M. Optimal dynamical range of excitable networks at criticality. *Nature Physics* **2**, 348–351 (2006).
- [13] Shew, W. L. & Plenz, D. The functional benefits of criticality in the cortex. *The Neuroscientist* **19**, 88–100 (2013).
- [14] Buzsaki, G. *Rhythms of the Brain* (Oxford University Press, USA, 2009).
- [15] Bertschinger, N. & Natschlagel, T. Real-time computation at the edge of chaos in recurrent neural networks. *Neural Computation* **16**, 1413–1436 (2004).
- [16] Jensen, H. J. *Self-organized criticality: emergent complex behavior in physical and biological systems* (Cambridge university press, 1998).
- [17] Pitt, D. Mental representation. In Zalta, E. N. (ed.) *The Stanford Encyclopedia of Philosophy* (2012), winter 2012 edn.
- [18] Edlund, J. A. *et al.* Integrated information increases with fitness in the evolution of animats. *PLoS Comput Biol* **7**, e1002236 (2011).
- [19] Marr, D. *Vision: A Computational Investigation into the Human Representation and Processing of Visual Information* (MIT press, 2010).

- [20] Attneave, F. Some informational aspects of visual perception. *Psychological review* **61**, 183–193 (1954).
- [21] Barlow, H. B. Possible principles underlying the transformation of sensory messages. *Sensory communication* 217–234 (1961).
- [22] Rieke, F., Bodnar, D. & Bialek, W. Naturalistic stimuli increase the rate and efficiency of information transmission by primary auditory afferents. *Proceedings of the Royal Society of London. Series B: Biological Sciences* **262**, 259–265 (1995).
- [23] Bialek, W., van Steveninck, R. R. R. & Tishby, N. Efficient representation as a design principle for neural coding and computation. *2006 IEEE International Symposium on Information Theory* 659–663 (2006).
- [24] Holland, J. H. *Adaptation in natural and artificial systems: an introductory analysis with applications to biology, control and artificial intelligence* (MIT press, 1992).
- [25] Nolfi, S. & Floreano, D. *Evolutionary robotics: The biology, intelligence, and technology of self-organizing machines* (MIT press, 2000).
- [26] Cover, T. M. & Thomas, J. *Elements of Information Theory* (Wiley, 1991).
- [27] Goldberg, D. E. *Genetic Algorithms in Search, Optimization, and Machine Learning* (Addison-Wesley Professional, 1989).
- [28] Gros, C. *Complex and adaptive dynamical systems: A primer* (Springer, 2008).
- [29] Mastromatteo, I. & Marsili, M. On the criticality of inferred models. *Journal of Statistical Mechanics: Theory and Experiment* **2011**, P10012 (2011).
- [30] Kauffman, S. *The origins of order: Self-organization and selection in evolution* (Oxford University Press, USA, 1993).
- [31] Goudarzi, A., Teuscher, C., Gulbahce, N. & Rohlf, T. Emergent criticality through adaptive information processing in boolean networks. *Physical Review Letters* **108**, 128702 (2012).

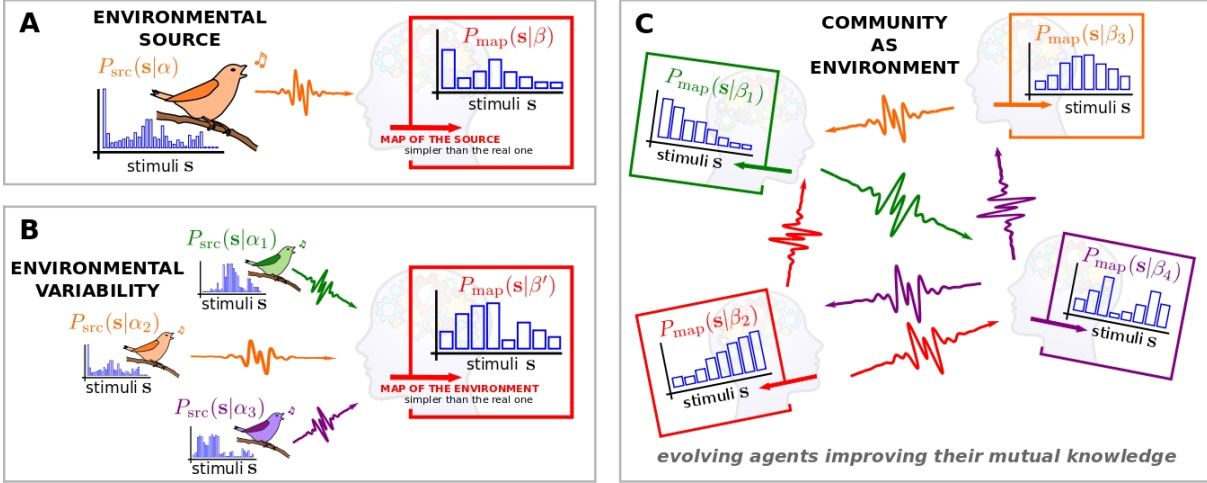


Figure 1: **Cognitive systems construct simplified maps of the environment.**

Panel A illustrates a *cognitive system* responding to an *environmental source* (e.g. a singing bird). The source can produce different stimuli  $s$ , represented by  $P_{src}(s|\alpha)$ , which quantifies the statistical properties of the stimuli (e.g. patterns of the bird song). A cognitive system maps the source by building an internal representation  $P_{map}(s|\beta)$ , simpler than  $P_{src}(s|\alpha)$ , aimed at capturing its most relevant features (e.g. most prominent notes or chorus). The optimal choice of parameters  $\beta$  is obtained by minimizing the Kullback-Leibler divergence of  $P_{map}(s|\beta)$  from  $P_{src}(s|\alpha)$ . Panel B shows a more complex panorama, in which the cognitive system has to cope with multiple sources simultaneously. In this case, the best choice of the map needs to account for the various sources the system is exposed to. For highly heterogeneous sources, we have found that the optimal parameter choice lies in the vicinity of a critical point. In panel C, the environment is composed of the cognitive systems themselves with each of them perceiving the others. The systems evolve as they map each other and generate a self-organized environment. We have developed computational models in which individual systems are subject to adaptive/evolutionary dynamics with the fittest individuals being those that can better map their environment. Remarkably, the evolution drives the parameters of the individuals very close to a critical point.

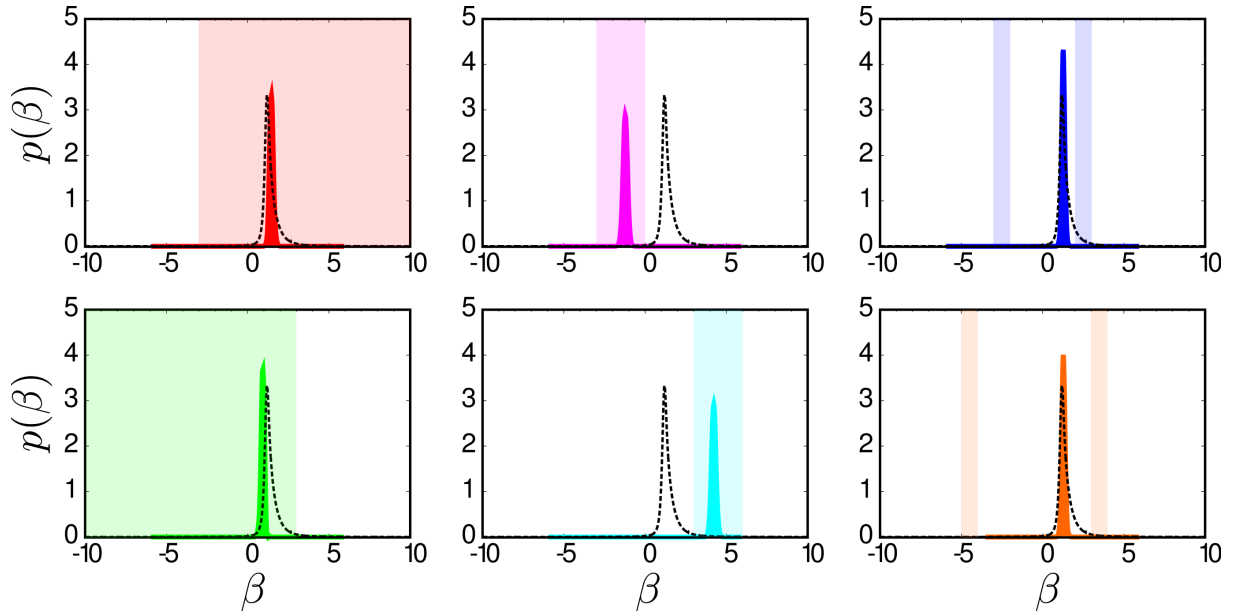


Figure 2: **Evolutionary model leading to criticality in complex environments.** A community of  $M$  cognitive systems (or agents) undergoes a genetic algorithm dynamics.<sup>27</sup> Each agent is simultaneously exposed to diverse stimuli  $\mathbf{s}$  provided by  $S$  different sources, each one characterized by a probability  $P_{src}(\mathbf{s}|\alpha^u)$  with  $u = 1, \dots, S$ , fully specified by parameters  $\alpha^u$ . At each time step,  $S$  sources are randomly drawn with probability  $\rho_{src}(\alpha^u)$  (in this case uniform with support in the colored region). Each agent  $i$  ( $i = 1, \dots, M$ ) constructs an internal representation  $P_{map}(\mathbf{s}|\beta^i)$  of the environment. Individuals' fitness increases as the mean Kullback-Leibler divergence from the set of sources to which they are exposed decreases (see eq. 1). The higher the fitness an agent has, the lower is its probability of dying. A death is replaced by a new agent with a parameter  $\beta$  inherited from one of the other agents (but with a small variation/mutation). The community dynamically evolves and eventually reaches a steady state distribution of parameters,  $p(\beta)$ . The six panels in the figure correspond to different supports for uniform source distributions,  $\rho_{src}(\alpha^u)$ . The dashed line is the generalized susceptibility (Fisher information) of the internal map, which exhibits a peak at the critical point. Heterogeneous source pools (left and right panels) lead to distributions peaked at criticality, whereas for homogeneous sources (center panels) communities are not critical but specialized. The stimuli distributions are parametrized as  $P_{src}(\mathbf{s}|\alpha^u) \propto \exp\{\alpha^u \frac{N}{2} (\sum_{k=1}^N \frac{s_k}{N})^2\}$  while the maps are identical but replacing  $\alpha_u$  by  $\beta_i$ . See Methods and SI for further details.

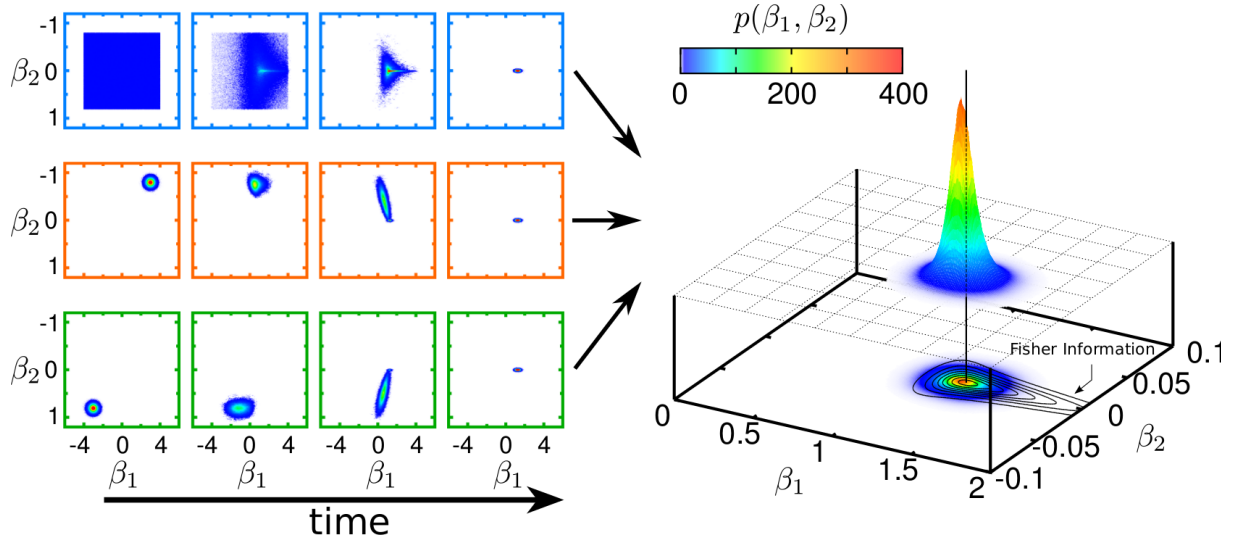


Figure 3: **Co-evolutionary model leads self-consistently to criticality:** A community of  $M$  cognitive systems (or agents) evolves according to a genetic algorithm dynamics.<sup>27</sup> Each individual is characterized by a 2-parameter  $(\beta_1, \beta_2)$  map and the rest of the community acts as the external environment it has to cope with, i.e. the agents try to “understand” each other (see Fig. 1 C) . At each simulation step, two individuals are randomly chosen and their respective fitnesses (i.e. Kullback-Leibler divergence from each other’s map) computed. One of the two agents is removed from the community with a probability that is smaller for the fitter agent with the winner producing an offspring which (except for small variations/mutations) inherits its parameters. These co-evolutionary rules drive the community very close to a unique localized steady state. As shown in the right panel, the steady state is localized precisely at the critical point, i.e. where the generalized susceptibility (or Fisher information) of the maps has a sharp peak (as shown by the contour plots). The map distributions are parameterized as  $P_{map}(\mathbf{s}|\beta_1, \beta_2) \propto \exp \{ \beta_1 \frac{N}{2} (\sum_{k=1}^N \frac{s_k}{N})^2 + \beta_2 \sum_{k=1}^N s_k \}$  (see Methods and SI for further details).

# Supplementary Information: Emergence of criticality in living systems through adaptation and evolution

J. Hidalgo, J. Grilli, S. Suweis, M.A. Muñoz, J.R. Banavar, and A. Maritan

## S1 Brief primer on critical phenomena

Critical phenomena are well understood in physical systems [1, 2]. The great lesson learnt from statistical physics is that, even though the elementary constituents can be as simple as spheres or spins sitting on a lattice with pair-wise interactions, criticality and scale invariance emerge as the collective behavior of a many-body system with its characteristics depending only on just a few essential attributes such as the dimensionality of the system and symmetries of the problem. Remarkably, this universality results in the critical behavior of an Ising model with nearest neighbor interactions on a cubic lattice being identical to that of a liquid-vapor system at its critical point. Likewise, the critical behavior of a binary alloy that is about to order is the very same as the two other cases. This is because all these systems are three dimensional and have the same “up-down” symmetry. The underlying details: the fact that spins sit on an idealized lattice, the chemistry of the liquid, or the atomic interactions in an alloy are irrelevant in determining the critical behavior.

A classical Ising spin can point up or down. An interaction between neighboring spins results in favoring a parallel relative orientation over an antiparallel one. This is captured through an interaction energy that is lower and thus more favorable when neighboring spins are parallel compared to when they are antiparallel. Note that our description of the model favors parallel over antiparallel but up and down are treated symmetrically. The ground state or the lowest energy state of such an Ising system is one in which all spins are parallel and, by necessity, are all up or all down. This choice between up and down breaks the up-down symmetry spontaneously. The advantage of lowering the energy through a mostly parallel alignment and thus breaking the symmetry, favored at low temperatures, competes with the tendency to increase the entropy at high temperatures through a restoration of the symmetry and having roughly equal numbers of up and down spins. While there are just two states with perfectly parallel spins –all up or all down– there are many states and therefore a higher entropy when approximately half the spins are up and the other half are down. The magnetization of such an Ising system is proportional to a suitably normalized imbalance between the numbers of up and down spins. It provides a measure of the ordering and is zero at high temperatures and is 1 at zero temperature. On lowering the temperature from a very high value, the magnetization remains zero until a critical temperature is reached at which point the magnetization rises continuously and becomes non-zero. The critical point is then a special temperature at which there is an onset of a non-zero magnetization and the up-down symmetry is spontaneously broken. There are two phases that emerge: at any temperature higher than  $T_c$ , the magnetization is zero for an infinite sized system whereas, below  $T_c$ , the magnetization is non-zero. The critical point, which separates these two phases, is obtained by tuning the temperature just right to its critical value. At a critical point, there are domains of up and down spins of all sizes thoroughly interspersed among one another. Scale invariance occurs because there is no dominant size scale associated with these domains and power law correlations between spin orientations are observed.

At the critical point, the system is exquisitely sensitive to external perturbations of the right sort. For example, imposing a magnetic field, whose tendency is to align the spins along the field direction, does not have a significant effect at very low temperatures because the spins are aligned parallel to each other and there is already a non-zero magnetization. A measure of this sensitivity is provided by the magnetic susceptibility,

which is a measure of a differential increase of magnetization due to an imposition of an infinitesimal magnetic field. As argued before, the susceptibility is small at low temperatures. It is also small at very high temperatures – thermal effects, which favor high entropy, do not encourage much alignment of the spins and imposing a tiny magnetic field does not lead to much alignment. As a function of temperature, the susceptibility shows a peak at the critical temperature. Remarkably, for an infinite system, the susceptibility becomes infinitely large at its critical point. For a finite size system, the position of the maximum of the susceptibility provides an excellent measure of the location of the critical point. We use a generalized susceptibility in the main text as a diagnostic of critical behavior.

A conjecture by Langton suggests that complex computations can be only performed by “machines” operating at the “edge of chaos”, i.e. at the borderline between the chaotic phase, in which perturbations and noise propagate unboundedly (thereby corrupting information), and the frozen phase whereas changes are rapidly erased (hindering the possibility for the system to react and limiting enormously its computing capability) [3, 4]. The edge of chaos –that for all purposes here is just the “critical region”, with its concomitant power-laws and scaling, in the statistical mechanics jargon– provides a delicate compromise between these two impractical tendencies [5, 6, 7]. In recent years, it has been suggested that critical dynamics leads to optimal computational capabilities[8], optimal transmission and storage of information [9], and maximal sensitivity to sensory stimuli [10]. Actually, empirical evidence has been flourishing that living systems (or parts, aspects or groups of them) do operate at the vicinity of critical points, with examples ranging from brain spontaneous activity [11], to resting time distributions of mice [12], gene expression patterns [13], cell growth [14], bacterial clustering [15], and flock dynamics [16] (a critical discussion of this issues can be found in [17]).

## S2 Kullback-Leibler divergence, maximum likelihood, and Sanov’s theorem

Given two probability distributions  $P(\mathbf{s})$  and  $Q(\mathbf{s})$  for the set of variables  $\mathbf{s}$ , the Kullback-Leibler (KL) divergence of  $Q(\mathbf{s})$  from  $P(\mathbf{s})$  is defined as

$$D(P(\cdot)|Q(\cdot)) := \sum_{\mathbf{s}} P(\mathbf{s}) \log\left(\frac{P(\mathbf{s})}{Q(\mathbf{s})}\right), \quad (\text{S1})$$

and quantifies the loss of information when  $Q(\mathbf{s})$  is used to approximate  $P(\mathbf{s})$  [18, 19]. The KL divergence is non-negative and it vanishes if and only if both distributions are equal. Observe also that the KL divergence is not symmetric and therefore is not a properly-defined “distance”.

The KL divergence can be understood in terms of the maximum likelihood principle or of the Sanov’s theorem [20, 19, 21]. Consider a long sequence of empirical data consisting of  $T$  independent measurements. Let  $C(\mathbf{s})$  be the number of times a certain event  $\mathbf{s}$  is repeated in the sequence. Suppose that events are distributed as  $P(\mathbf{s})$ . In the large  $T$  limit, the frequencies  $C(\mathbf{s})/T$  converge to  $P(\mathbf{s})$ , by the Glivenko-Cantelli theorem. A model for a finite sampling of size  $T$  can be represented as a probability distribution  $Q(\mathbf{s})$ . The (multinomial) likelihood is defined as

$$\mathcal{L} = \frac{T!}{\prod_{\mathbf{s}} C(\mathbf{s})!} \prod_{\mathbf{s}} Q(\mathbf{s})^{C(\mathbf{s})}, \quad (\text{S2})$$

which is nothing but the probability that the model  $Q(\mathbf{s})$  generates a sequence of  $T$  observations compatible with  $C(\mathbf{s})$ . The previous equation can be rewritten as

$$\mathcal{L} = T! \exp \sum_{\mathbf{s}} \left( C(\mathbf{s}) \log(Q(\mathbf{s})) - \log(C(\mathbf{s})!) \right), \quad (\text{S3})$$

which, in the large  $T$  limit, using the approximations  $T! \sim T^T$  and  $C(\mathbf{s}) \sim TP(\mathbf{s})$  becomes

$$\mathcal{L} \sim \exp\left(-T \sum_{\mathbf{s}} D(P(\mathbf{s})|Q(\mathbf{s}))\right) \quad (\text{S4})$$

up to leading order. Therefore, maximizing the likelihood of a trial probability distribution function  $Q$  is equivalent to minimizing its KL divergence with respect to the original one,  $P$ . This result is also known as Sanov’s theorem [20] in the context of large deviations theory.



### S3 Mapping the external world

A signal provided by the environment (called a “source” from now on) can be modeled by a set of  $N$  binary variables  $\mathbf{s} = (s_1, s_2, \dots, s_N)$ , where  $s_i = \pm 1, \forall i$ . Signals  $\mathbf{s}$  are distributed with a suitable  $P_{src}(\mathbf{s}|\boldsymbol{\alpha})$ , which specifies the statistical properties of stimuli and depends on some “environmental” parameters  $\boldsymbol{\alpha} = (\alpha_1, \alpha_2, \dots, \alpha_E)$ .

Without loss of generality, it is possible to write

$$P_{src}(\mathbf{s}|\boldsymbol{\alpha}) = \frac{\exp(-H_{src}(\mathbf{s}|\boldsymbol{\alpha}))}{Z_{src}(\boldsymbol{\alpha})}, \quad (\text{S5})$$

which defines  $H_{src}$  up to a constant, independent of  $\mathbf{s}$ , which can be set equal to zero. The factor  $Z_{src}(\boldsymbol{\alpha})$  is defined by normalization condition. The quantity  $H_{src}$  can be expressed as

$$H_{src}(\mathbf{s}|\boldsymbol{\alpha}) = \sum_{\mu=1}^E \alpha_{\mu} \phi_{src}^{\mu}(\mathbf{s}), \quad (\text{S6})$$

where  $E$  is the number of parameters specifying the source and  $\phi^{\mu}(\mathbf{s})$  are suitable functions (“observables”). Equations S5 and S6 are a convenient parametrization of the probability distribution function, so that different values of  $\boldsymbol{\alpha}$  specify distinct source distributions  $P_{src}$ .

A “cognitive system” is characterized by a set of internal parameters  $\boldsymbol{\beta} = (\beta_1, \beta_2, \dots, \beta_I)$  which represents a *map* (i.e. a simplified description) of the perceived signal,  $P_{map}(\mathbf{s}|\boldsymbol{\beta})$ , and which –in analogy with eq. S5– can be written as

$$P_{map}(\mathbf{s}|\boldsymbol{\beta}) = \frac{\exp(-H_{map}(\mathbf{s}|\boldsymbol{\beta}))}{Z_{map}(\boldsymbol{\beta})}, \quad (\text{S7})$$

where

$$H_{map}(\mathbf{s}|\boldsymbol{\beta}) = \sum_{\mu=1}^I \beta_{\mu} \phi_{map}^{\mu}(\mathbf{s}) \quad (\text{S8})$$

where  $I$  is the number of “internal” (or map) parameters.

Information theory provides us with a natural tool to characterize an optimal choice of  $\boldsymbol{\beta}$  for a given  $\boldsymbol{\alpha}$ . In particular, the Kullback-Leibler (KL) divergence (see section S2) quantifies the amount of information lost when a probability distribution is approximated by another one. Minimizing the Kullback-Leibler divergence between the “source” and “internal” distributions leads to the following general relation between the source’s parameters  $\boldsymbol{\alpha}$  and the optimal choice for the internal map parameter set

$$\boldsymbol{\beta} = \mathbf{L}(\boldsymbol{\alpha}) = \arg \min_{\boldsymbol{\beta}'} D(\boldsymbol{\alpha}|\boldsymbol{\beta}'), \quad (\text{S9})$$

where  $D(\boldsymbol{\alpha}|\boldsymbol{\beta})$  is the KL divergence of equations S5 and S7. The ability to cope –even if in an optimal way– with a single and precise environmental source is not enough to cope with a complex and changing world. Therefore, we need to introduce a last key ingredient: *environmental variability*. In order to account for broadly diverse and variable external sources,  $\boldsymbol{\alpha}$ , we introduce a probability density of different parameter sets  $\rho_{src}(\boldsymbol{\alpha})$ , which describes the variability of  $\boldsymbol{\alpha}$  or the probability to encounter a source with a given choice of parameters.

### S4 Analytical results I: General theory

The KL divergence between the distributions characterized by generic parameter sets  $\boldsymbol{\alpha}$  and  $\boldsymbol{\beta}$  respectively,  $D(\boldsymbol{\alpha}|\boldsymbol{\beta}) = D(P_{src}(\cdot|\boldsymbol{\alpha})|P_{map}(\cdot|\boldsymbol{\beta}))$ , can be easily written by using the generic parametrization of equations S5 and S7:

$$D(\boldsymbol{\alpha}|\boldsymbol{\beta}) = \sum_{\mu=1}^I \beta_{\mu} \langle \phi_{map}^{\mu} \rangle_{\boldsymbol{\alpha}} + \log Z_{map}(\boldsymbol{\beta}) - S_{src}(\boldsymbol{\alpha}), \quad (\text{S10})$$

with

$$\begin{aligned} \langle \phi_{map}^\mu \rangle_{\alpha} &:= \sum_{\mathbf{s}} \phi_{map}^\mu(\mathbf{s}) P_{src}(\mathbf{s}|\alpha) \\ S_{src}(\alpha) &:= - \sum_{\mathbf{s}} P_{src}(\mathbf{s}|\alpha) \log(P_{src}(\mathbf{s}|\alpha)) , \end{aligned} \quad (\text{S11})$$

where the last expression is the entropy of the distribution  $P_{src}$ .

To proceed further, there are two alternative ways to define the optimal choice of parameter  $\beta$  given the distribution of external parameters  $\rho_{src}(\alpha)$ .

In the first one (to which we will refer as ‘‘quenched’’ choice), we construct a map for every source, characterized by  $\alpha$ , by minimizing the KL divergence with respect to  $\beta$ , and then we compute the distribution of maps  $\rho_{map}(\beta)$ . The optimal choice,  $\beta_q^{\text{opt}}$ , corresponds to the maximum value of  $\rho_{map}$ , i.e. the value of  $\beta$  which maps the higher number of sources. Mathematically, it can be express as

$$\beta_q^{\text{opt}} = \arg \max_{\beta} \left[ \int d\alpha \delta(\beta - \arg \min_{\beta'} D(\alpha|\beta')) \rho_{src}(\alpha) \right] , \quad (\text{S12})$$

Instead, in the second (‘‘annealed’’) case we compute the value of  $\beta$  which has a lower average KL divergence over the parameters  $\alpha$ . Formally, it is written as

$$\beta_a^{\text{opt}} = \arg \min_{\beta} \left[ \int d\alpha D(\alpha|\beta) \rho_{src}(\alpha) \right] \quad (\text{S13})$$

and the system adopts the single value of  $\beta$ ,  $\beta_a^{\text{opt}}$ , that better describes *on average* the varying environment.

#### S4.1 Quenched choice

Given a set of parameters  $\alpha$  characterizing the source, the optimal mapping  $\mathbf{L}(\alpha)$  is defined by eq. S9. By using eq. S10, one readily obtains the equations for the stationary points (extrema) of the KL divergence

$$0 = \frac{\partial}{\partial \beta_\mu} D(\alpha|\beta) = \langle \phi_{map}^\mu \rangle_{\alpha} - \langle \phi_{map}^\mu \rangle_{\beta} , \quad (\text{S14})$$

with the index  $\mu$  running from 1 to  $I$  and  $\langle \phi_{map}^\mu \rangle_{\beta} := \sum_{\mathbf{s}} \phi_{map}^\mu(\mathbf{s}) P_{map}(\mathbf{s}|\beta)$ .

To check whether extrema are minima or maxima, one needs to evaluate the Hessian matrix at the stationary point,

$$\frac{\partial^2}{\partial \beta_\mu \partial \beta_\nu} D(\alpha|\beta) = - \frac{\partial}{\partial \beta_\nu} \langle \phi_{map}^\mu \rangle_{\beta} = \langle \phi_{map}^\mu \phi_{map}^\nu \rangle_{\beta} - \langle \phi_{map}^\mu \rangle_{\beta} \langle \phi_{map}^\nu \rangle_{\beta} \equiv \langle \langle \phi_{map}^\mu \phi_{map}^\nu \rangle \rangle_{\beta} , \quad (\text{S15})$$

which is a positive defined matrix (excluding the trivial case of a factorized  $P_{map}(\mathbf{s}|\beta)$  for which it vanishes). Therefore, if the solution of eq. S14 exists, it corresponds to minimum of the KL divergence. Equation S14, which implicitly defines the optimal map  $\beta = \mathbf{L}(\alpha)$ , has an intuitive interpretation: *the minimum of the KL divergence is obtained when the first  $I$  moments of the distribution  $P_{map}(\mathbf{s}|\beta)$  exactly match those of  $P_{src}(\mathbf{s}|\alpha)$ .*

Therefore, the internal parameters are uniquely fixed via the optimal map Eq.S14 given the internal ones. If we introduce a distribution of external parameters  $\rho_{src}(\alpha)$  it is straightforward to obtain a distribution of internal parameters  $\rho_{map}(\beta)$ , defined in the following way

$$\rho_{map}(\beta) := \int d\alpha \rho_{src}(\alpha) \delta(\beta - \mathbf{L}(\alpha)) . \quad (\text{S16})$$

One can show that this distribution is proportional to the *Fisher information* or *generalized susceptibility* of the internal system,

$$\chi_{map}^{\mu\nu}(\beta) := - \frac{\partial}{\partial \beta_\mu} \langle \phi_{map}^\mu \rangle_{\beta} = \langle \langle \phi_{map}^\mu \phi_{map}^\nu \rangle \rangle_{\beta} , \quad (\text{S17})$$

which diverges at the critical point in the limit  $N \rightarrow \infty$ . When the external parameters are not centered about a critical point, the distribution  $\rho_{map}(\beta)$  will peak at the critical point at large but finite  $N$ .

## S4.2 Annealed choice

Here we analyze the model defined via eq. S13. In this case, the optimal choice corresponds to the value of the internal parameter  $\beta$  which minimizes the average KL divergence to the sources  $\alpha$ , defined as

$$d(\rho_{src}|\beta) := \int d\alpha \rho_{src}(\alpha) D(\alpha|\beta) . \quad (\text{S18})$$

Plugging the specific expression for the KL divergence, i.e. equation S10, into this, we obtain an equation for the stationary points:

$$0 = \frac{\partial}{\partial \beta_\mu} d(\rho_{src}|\beta) = -\langle \phi_{map}^\mu \rangle_\beta + \int d\alpha \rho_{src}(\alpha) \langle \phi_{map}^\mu \rangle_\alpha . \quad (\text{S19})$$

This equation can be interpreted in an alternative way; introducing the ‘‘averaged environment’’

$$\bar{P}_{src}(\mathbf{s}|\rho_{src}) := \int d\alpha \rho_{src}(\alpha) P_{src}(\mathbf{s}|\alpha) , \quad (\text{S20})$$

the KL divergence respect to  $P_{map}(\mathbf{s}|\beta)$  is

$$D(\bar{P}_{src}(\cdot|\rho_{src})|P_{map}(\cdot|\beta)) = d(\rho_{src}|\beta) - \int d\alpha \rho_{src}(\alpha) D(P_{src}(\cdot|\alpha)|\bar{P}_{src}(\cdot|\rho_{src})) . \quad (\text{S21})$$

Since the last term on the right hand side does not depend on  $\beta$ , the minimization of the KL divergence between the ‘‘averaged environment’’ and the internal mapping  $P_{src}(\mathbf{s}|\beta)$  leads to the same result as the minimization of  $d(\rho_{src}|\beta)$  given by eq. S18. In both cases, the Hessian matrix turns out to be strictly positive (see equation S15), and therefore the eventual extrema are local minima.

In the particular case in which  $I = E$ , writing  $\phi_{src}^\mu = \phi_{map}^\mu = \phi^\mu$ , the optimal mapping  $\beta$  is given by the solution of eq. (S19), which can be simply written as

$$\langle \phi^\mu \rangle_\beta = \int d\alpha \rho_{src}(\alpha) \langle \phi^\mu \rangle_\alpha . \quad (\text{S22})$$

To illustrate this result we consider a system characterized by only one parameter  $\alpha$  and by a bounded  $\phi$ . We assume that a phase transition occurs at  $\alpha = \alpha_c$  and for simplicity  $\langle \phi \rangle_\alpha$  has a sigmoid shape with an inflection point at  $\alpha = \alpha_c$  with a tangent becoming more and more vertical as  $N$  increases. If  $\rho_{src}(\alpha)$  is uniform in the interval  $(\bar{\alpha} - a, \bar{\alpha} + a)$ , we want to determine the direction in which  $\beta$  moves with respect to the relative position of  $\bar{\alpha}$  with respect to  $\alpha_c$  where  $\beta^{\text{opt}}$  is the optimal value obtained with equation S22. In the limit of small interval size  $a$  we obtain

$$\langle \phi \rangle_\beta = \int_{\bar{\alpha}-a}^{\bar{\alpha}+a} d\alpha \frac{1}{2a} \langle \phi \rangle_\alpha \sim \langle \phi \rangle_{\bar{\alpha}} + \langle \phi \rangle_{\bar{\alpha}}'' \frac{a^2}{6} , \quad (\text{S23})$$

where  $\langle \phi \rangle_{\bar{\alpha}}''$  is the second derivative of  $\langle \phi \rangle_\alpha$  evaluated in  $\bar{\alpha}$ . Expanding the left hand side of the equation around  $\bar{\alpha}$  we get

$$\beta - \bar{\alpha} \sim \frac{\langle \phi \rangle_{\bar{\alpha}}''}{\langle \phi \rangle_{\bar{\alpha}}'} \frac{a^2}{6} . \quad (\text{S24})$$

If the sigmoid shape has a positive (negative) derivative, then the second derivative will be positive (negative) below the critical point and negative (positive) above, leading to  $\beta^{\text{opt}} > \bar{\alpha}$  if  $\bar{\alpha} < \alpha_c$  and  $\beta^{\text{opt}} < \bar{\alpha}$  if  $\bar{\alpha} > \alpha_c$ .

This result can be generalized to the case of a multi dimensional parameters space. One can indeed introduce a scalar quantity which is peaked at the critical point, and show that the projection of the vector  $\beta - \bar{\alpha}$  on the gradient of this quantity is always positive, and therefore that the optimal parameter is ‘‘closer’’ to the critical point.

## S5 Analytical results II: Examples

### S5.1 Quenched choice

We analyze numerically a simple case, inspired by the archetypical (mean-field) Ising model [2], in which

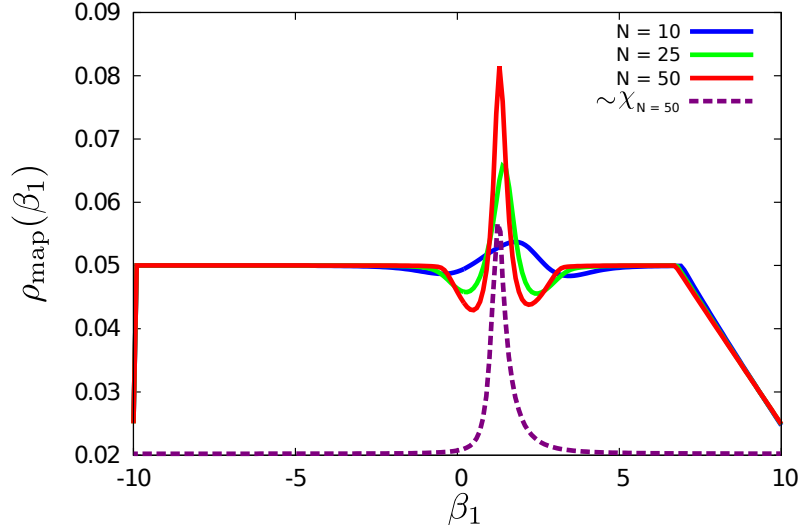
$$H_{src}(\mathbf{s}|\boldsymbol{\alpha}) = -\frac{N}{2}\alpha_1 \left( \sum_i \frac{s_i}{N} \right)^2 - \frac{N}{4!}\alpha_2 \left( \sum_i \frac{s_i}{N} \right)^4 \quad (\text{S25})$$

and

$$H_{map}(\mathbf{s}|\boldsymbol{\beta}) = -\frac{N}{2}\beta_1 \left( \sum_i \frac{s_i}{N} \right)^2 = -\frac{1}{N}\beta_1 \sum_{i,j>i}^N s_i s_j + \text{constant}. \quad (\text{S26})$$

Numerical factors  $(-N/2)$  and  $(-N/4!)$  have been introduced for convenience. The last form of the  $H_{map}$  visually relates this internal mapping with the classic problem of Boltzmann learning [22].

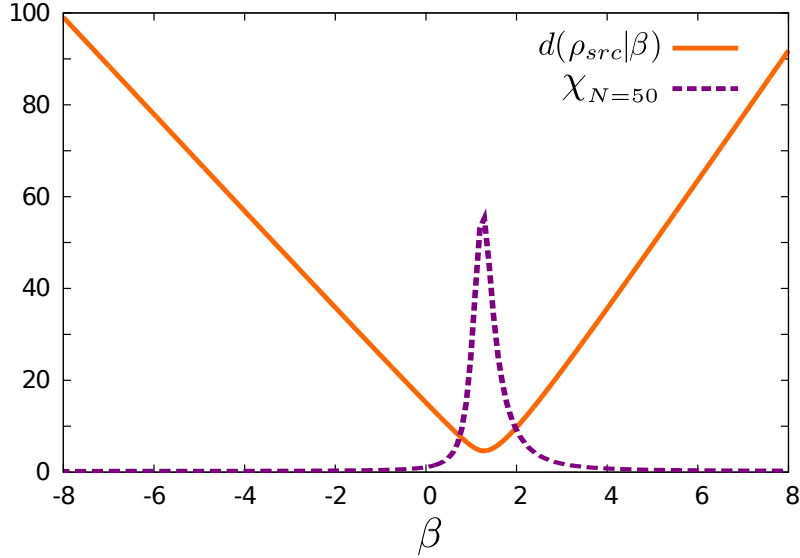
As explained in section S4.1, we take a specific distribution  $\rho_{src}(\boldsymbol{\alpha})$  –in this case a uniform distribution in the range  $(\alpha_1, \alpha_2) \in [-10, 10] \times [-20, 20]$ – and we compute the map distribution  $\rho_{map}(\boldsymbol{\beta})$ . The result is shown in Fig. S1 together with the corresponding generalized susceptibility, for different values of  $N$ ,



**Supplementary Figure S1:** *Quenched choice:*  $\rho_{map}(\beta_1)$  for source and individual parametrizations given in eq. S25 and S26, respectively. In this case, we choose  $\rho_{src}(\alpha_1, \alpha_2)$  to be uniform in the range  $[-10, 10] \times [-20, 20]$ . Colored solid lines represent  $\rho_{map}(\beta_1)$  for different values of  $N$ , while the dashed line is proportional to the generalized susceptibility of the model (as defined by eq. S17, for  $N = 50$ , and rescaled for visualization purposes). The maximum of this distribution, which turns out to be located very near the peak of the susceptibility, represents the optimal mapping, as given in eq. S12.

## S5.2 Annealed model

We now study a particular case of the theory developed in section S4.2. The difference respect to the previous case is that, here, we compute the mean distance of every map  $\beta$  respect to all the sources  $\alpha$ . Now, both the sources and the maps are modelled by eq.S26, each one containing only one parameter. In this case, we considered  $\rho_{src}(\alpha)$  uniform in the range  $(-10, 10)$ . The result of the mean distance as a function of  $\beta$  is plotted in Fig. S2.



**Supplementary Figure S2:** *Annealed choice.* The orange line is the average KL divergence  $d(\rho_{src}|\beta)$  of internal parameter  $\beta$ , defined in eq. S18. The dashed line is proportional to the of susceptibility of internal model (defined in eq. S17). The minimum of the distance is located close to the critical point (defined by the peak of the determinant of susceptibility). In this case both the source and the map are modelled by equation S26 with  $N = 50$ , and the source parameters are uniformly distributed in the range  $[-10, 10]$ .

## S6 Evolutionary models

We study the dynamics of two different evolutionary models, both of them inspired by a genetic algorithm [23, 24]. The first one consists of an ensemble of  $M$  individuals evolving in a world providing varying “external” stimuli. On the other hand, in the Co-evolutionary Model, individuals evolve with a similar algorithm but instead of having to cope with an external environment the community itself plays the role of the external world, i.e. individuals need to map the state of other similar individuals. We have studied different variants of this general model (see below).

### S6.1 Evolutionary Model

We model a community of individuals receiving external stimuli from an outer and heterogeneous environment. We describe every source of the environment by a generic distribution, as parametrized by equation S5 with

$$H_{src}(\mathbf{s}|\boldsymbol{\alpha}) = \sum_{\mu}^E \alpha_{\mu} \phi_{src}^{\mu}(\mathbf{s}), \quad (\text{S27})$$

where the parameters  $\boldsymbol{\alpha}$  are drawn from the distribution  $\rho_{src}(\boldsymbol{\alpha})$ .

In the community, each agent has a representation of the observed source (constructed as explained in previous sections). The map of the  $k$ -th agent is modelled with an internal system described by equation S7, with

$$H_{map}(\mathbf{s}|\boldsymbol{\beta}^k) = \sum_{\nu}^I \beta_{\nu}^k \phi_{map}^{\nu}(\mathbf{s}), \quad (\text{S28})$$

We consider the following dynamics:

1. We start with  $M$  individuals each one equipped with some initial parameter set extracted from some arbitrary (broad) distribution.  $p(\boldsymbol{\beta}, t = 0)$ .
2. At every time step, we generate  $S$  external sources,  $\{\boldsymbol{\alpha}^u\}_{u=1, \dots, S}$ , from the distribution  $\rho_{src}(\boldsymbol{\alpha})$ .
3. We compute the average KL divergence of every individual’s mapping to the external sources

$$d(\{\boldsymbol{\alpha}^u\}|\boldsymbol{\beta}^k) := \frac{1}{S} \sum_{u=1}^S \sum_{\mathbf{s}} P_{src}(\mathbf{s}|\boldsymbol{\alpha}^u) \log \frac{P_{src}(\mathbf{s}|\boldsymbol{\alpha}^u)}{P_{map}(\mathbf{s}|\boldsymbol{\beta}^k)}. \quad (\text{S29})$$

4. One of the individuals of the community is removed with a probability proportional to its average KL divergence

$$P_{kill}(k) = \frac{d(\{\boldsymbol{\alpha}^u\}|\boldsymbol{\beta}^k)}{\sum_l d(\{\boldsymbol{\alpha}^u\}|\boldsymbol{\beta}^l)} \quad (\text{S30})$$

and it is replaced by a copy of another individual (offspring), which is picked randomly with uniform probability.

5. The offspring inherits its parameter set from its parent or, instead, mutates with a probability  $\nu$ , altering the original parameter set,  $\boldsymbol{\beta} \rightarrow \boldsymbol{\beta} + \boldsymbol{\xi}$ , where  $\boldsymbol{\xi}$  is a random Gaussian number of zero mean and deviation  $\boldsymbol{\sigma}$ .
6. Time is incremented as  $t \rightarrow t + 1/M$ .
7. Another set of parameters  $\{\boldsymbol{\alpha}^u\}_{u=1, \dots, S}$  is generated from  $\rho_{src}(\boldsymbol{\alpha})$ , and the process is iterated.

We are interested in measuring the stationary distribution of the individual parameters,  $p(\boldsymbol{\beta}) \equiv p(\boldsymbol{\beta}, t \rightarrow \infty)$  when  $t \rightarrow \infty$  (we start measuring at some time  $T_i$  and stop at time  $T_f$ ), for which the distribution is averaged over  $R$  independent realizations of the initial distribution  $p(\boldsymbol{\beta}, t = 0)$ .

We have simulated the simple case in which both the external sources and internal maps correspond to the simple choice given in equation S25 with  $\alpha_2 = 0$  and equation S26 respectively. Similar results can be obtained for other parametrization of sources and maps, for instance by considering equation S25 with non-vanishing  $\alpha_2$ .

## Numerical computation of the Kullback-Leibler divergence

We explore the dependence of the stationary distribution  $p(\boldsymbol{\beta})$  on parameter values (see Table S1).

Parameter	Value
$N$	100
$M$	100
$S$	10
$\nu$	0.1
$\sigma$	0.1
$\rho_{src}(\alpha_1)$ (not used in Fig. 2 of main text)	$U([-10, 10])$
$T_i$	$10^4$
$T_f - T_i$	$10^5$
$R$	100

**Supplementary Table S1:** Parameters of the simulation of the Evolutionary Model in Fig. 2 of the main text and Fig. S3:  $N$  is the number of spins composing each of the individuals,  $M$  is the community size,  $S$  is the number of stimuli received in every interaction with the environment,  $\nu$  is the mutation probability,  $\sigma$  is the deviation of the mutated offspring,  $T_i$  and  $T_f$  are the initial and final time steps used for the measure and  $R$  is the number of independent realizations.

For sufficiently large values of  $N$ , the sum in eq. S29 cannot be explicitly compute because of the diverging large number of states,  $2^N$ . However, since equations S26 and S25 depend on  $\mathbf{s}$  only through the magnetization  $m = \sum_i s_i/N$ ,

$$H_{src}(\mathbf{s}|\boldsymbol{\alpha}) = -\frac{N}{2}\alpha_1 m^2 \quad (\text{S31})$$

and

$$H_{map}(\mathbf{s}|\boldsymbol{\beta}) = -\frac{N}{2}\beta_1 m^2, \quad (\text{S32})$$

we can compute the sum as follows. Defining  $\Gamma(m)$  as the number of states with  $\sum_i s_i/N = m$ , and using the Stirling approximation, one readily obtains:

$$\Gamma(m) = \binom{N}{\frac{N(1+m)}{2}} \underset{N \gg 1}{=} \exp \left\{ -N \left( \frac{1+m}{2} \log \frac{1+m}{2} + \frac{1-m}{2} \log \frac{1-m}{2} \right) \right\}. \quad (\text{S33})$$

Then, the KL divergence can be computed as

$$D(\boldsymbol{\alpha}|\boldsymbol{\beta}) \underset{N \gg 1}{=} \int_{-1}^1 \Gamma(m) \frac{\hat{P}_{src}(m|\boldsymbol{\alpha})}{\hat{P}_{map}(m|\boldsymbol{\beta})} \log \frac{\hat{P}_{src}(m|\boldsymbol{\alpha})}{\hat{P}_{map}(m|\boldsymbol{\beta})} dm. \quad (\text{S34})$$

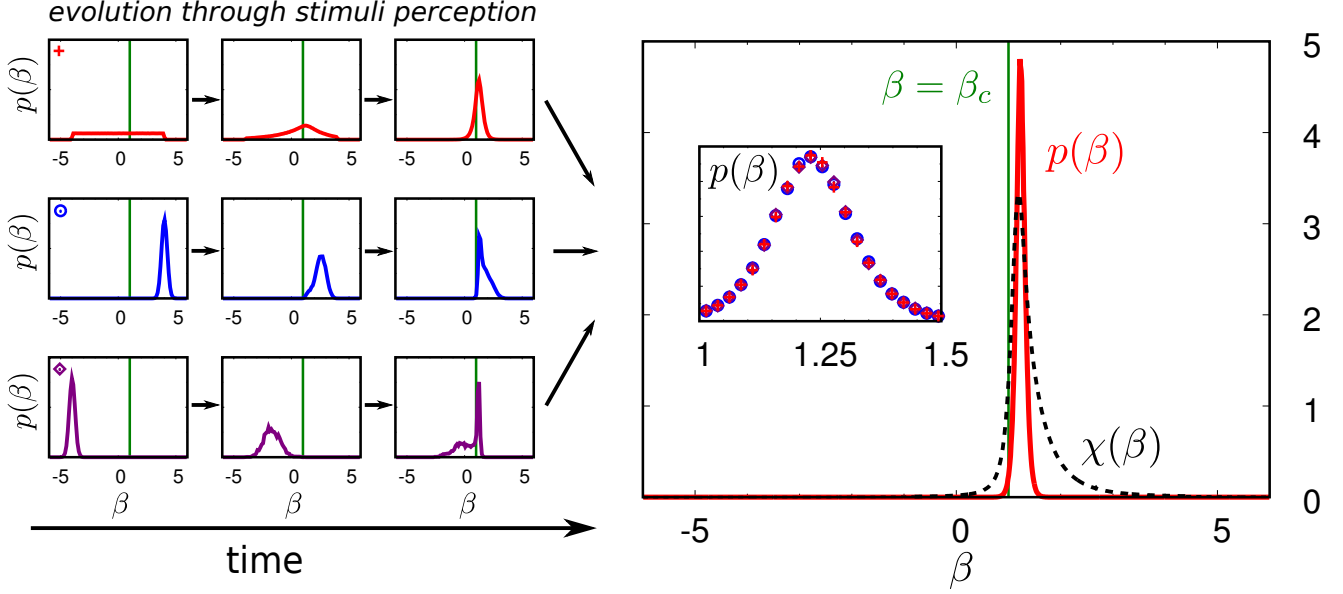
The same type of approximation can be used to calculate the normalization of  $P_{src}$  and  $P_{map}$ .

### S6.1.1 Results

Having computed the KL as a function of parameter values we can iterate the evolutionary dynamics, as described before. Figure S3 illustrates that starting from different initial conditions  $p(\boldsymbol{\beta}, 0)$  after some (sufficiently

long) times the ensemble of individuals converges to a unique steady state  $p(\beta, t \rightarrow \infty)$ . The resulting distribution is sharply peaked very near the critical point, at the very same location at which the Fisher information or generalized susceptibility peaks. This peak approaches the critical point  $\beta = \beta_c$  in the limit  $N \rightarrow \infty$ .

First, we proceed to analyze the relaxation of the initial distribution of parameters  $p(\beta, t = 0)$  at the stationary one  $p(\beta)$ , and its dependence on the initial condition. These results are plotted in Fig. S3. Fig. S4 illustrates the dependence of the results on parameters.

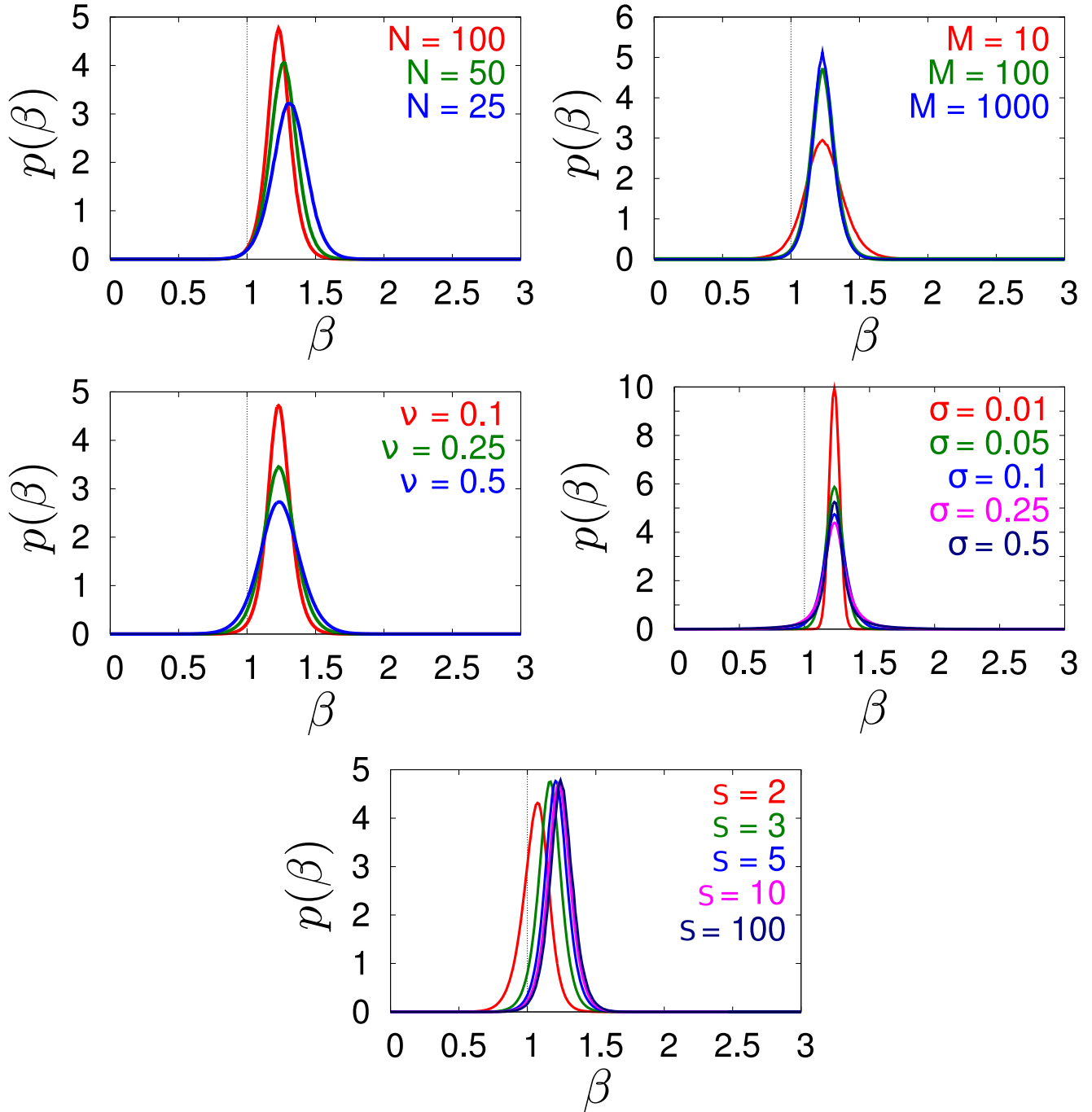


**Supplementary Figure S3:** *Time evolution in the Evolutionary Model* (with parametrization of eq. S25 with  $\alpha_2 = 0$  and eq. S26): Panels on the left represent the evolution of three different initial distributions of the parameter  $\beta$  in the community. In all cases the environment is described by the uniform distribution of parameters  $\rho_{src}(\alpha) = U([-10, 10])$ . The distributions converge to the same stationary state –points and red line on the right panel–, which is peaked at the maximum of the generalized susceptibility (dashed line curve). The red line corresponds to an initial uniform distribution  $U([-4, 4])$ , and blue and purple lines to Gaussian distributions  $N(4, 0.25)$  and  $N(-4, 0.25)$ , respectively. Parameters are the same as in Table S1, and  $R = 10^4$  independent realizations.

The main conclusions are:

- The system becomes closer and closer to the critical point as the system-size  $N$  is enlarged.
- The distribution reaches an asymptotic shape as the ensemble size grows.
- The distribution becomes sharper for smaller mutation rates.
- The distribution becomes much sharper for small mutation variances.
- The distribution reaches an asymptotic shape as the number of external sources is increased.





**Supplementary Figure S4:** *Dependence on parameters in the Evolutionary Model:* Stationary distribution  $p(\beta)$  as a function of diverse parameters; different colors in each plot stand for different values of (from top to bottom and from left to right):  $N$ , community size  $M$ , mutation probability  $\nu$ , mutation deviation  $\sigma$ , and number of external sources  $S$ . Unless otherwise stated, other parameters take the same values as in Table S1. The dashed lines indicate the critical point location (in the limit  $N \rightarrow \infty$ )

## S6.2 Co-evolutionary Model

Here we discuss a second type of evolutionary model, in which every individual receives stimuli from its surrounding world, which is nothing but the set of the other individuals in the community. More specifically: the  $k$ -th agent of the community is described by a probability distribution  $P_{map}(\mathbf{s}|\beta^k) \propto \exp\{-H_{map}(\mathbf{s}|\beta^k)\}$ , depending on parameters  $\beta^k$ .

Starting with an ensemble of  $M$  individuals whose coupling parameters are extracted from an arbitrary distri-

bution,  $p(\boldsymbol{\beta}, t = 0)$ , the evolutionary dynamics proceeds as follows:

1. At each time step, two individuals,  $i$  and  $j$ , are randomly selected.
2. Their relative fitnesses  $f_i$  and  $f_j$ , defined as the complementary KL divergences from the one to the other:

$$f_i = D(\boldsymbol{\beta}^i | \boldsymbol{\beta}^j) = \sum_{\mathbf{s}} P_{map}(\mathbf{s} | \boldsymbol{\beta}^i) \log \frac{P_{map}(\mathbf{s} | \boldsymbol{\beta}^i)}{P_{map}(\mathbf{s} | \boldsymbol{\beta}^j)}, \quad f_j = D(\boldsymbol{\beta}^j | \boldsymbol{\beta}^i) = \sum_{\mathbf{s}} P_{map}(\mathbf{s} | \boldsymbol{\beta}^j) \log \frac{P_{map}(\mathbf{s} | \boldsymbol{\beta}^j)}{P_{map}(\mathbf{s} | \boldsymbol{\beta}^i)}, \quad (\text{S35})$$

where –as the KL divergence is not symmetric–  $f_i \neq f_j$  unless  $\boldsymbol{\beta}^i = \boldsymbol{\beta}^j$ .

3. One of the two individuals –selected with probability proportional to its relative fitness– creates an offspring, while the other one is removed from the community.
4. As in the Evolutionary Model, the offspring inherits its parameters from its ancestor (with prob.  $1 - \nu$ ) or mutates with a probability  $\nu$ , modifying its parameters from  $\boldsymbol{\beta}$  to  $\boldsymbol{\beta} \rightarrow \boldsymbol{\beta} + \boldsymbol{\xi}$ , where  $\boldsymbol{\xi}$  is randomly chosen from a multivariate Gaussian distribution with zero mean and deviation  $\boldsymbol{\sigma}$ .
5. Time is updated to  $t \rightarrow t + 1/M$ .
6. Another couple of individuals  $i'$  and  $j'$  is picked, and the process is iterated.

To compute the stationary distribution of parameters  $p(\boldsymbol{\beta}) \equiv p(\boldsymbol{\beta}, t \rightarrow \infty)$ , we iterate  $T_i$  time steps and then perform measurements during  $T_f - T_i$  steps. Results are averaged over  $R$  realizations of the evolutionary process.

We now present some specific realizations of these general co-evolutionary rules. The “internal” probability distributions of a single individual are taken to as

$$H_{map}(\mathbf{s} | \boldsymbol{\beta}) = -\frac{N}{2}\beta_1 \left( \sum_i \frac{s_i}{N} \right)^2 - N\beta_2 \left( \sum_i \frac{s_i}{N} \right) \quad (\text{S36})$$

with a linear and a quadratic coupling. We will also discuss the simpler, particular case in which  $\beta_2$  vanishes (i.e. only the quadratic coupling is present), as well as the quadratic-quartic case:

$$H_{map}(\mathbf{s} | \boldsymbol{\beta}) = -\frac{N}{2}\beta_1 \left( \sum_i \frac{s_i}{N} \right)^2 - \frac{N}{4!}\beta_2 \left( \sum_i \frac{s_i}{N} \right)^4 \quad (\text{S37})$$

Figure 3 of the main text, shows the distribution of individual parameters,  $p(\boldsymbol{\beta})$  for the linear-quadratic case, eq. S36, for three different initial distributions and different transient periods, together with the final stationary distribution which is the same for all of them. Numerical parameters are summarized in Table S2.

### S6.2.1 Results

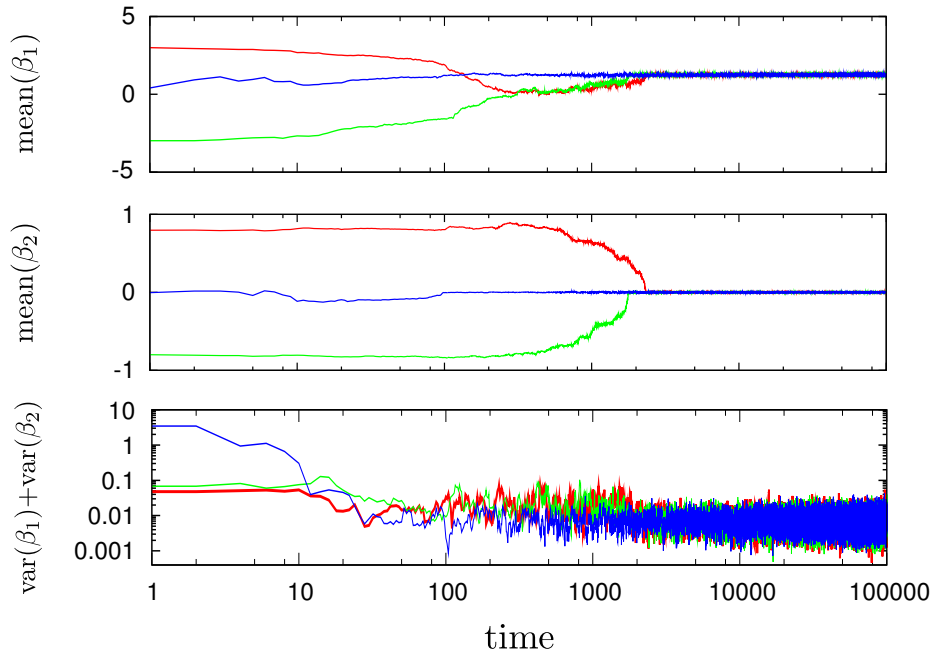
As for the Evolutionary Model, we first study the stationarity of the final distribution of parameters  $\boldsymbol{\beta}$  in the community and its dependence on number of spins,  $N$ , number of individuals,  $M$ , the mutation probability,  $\nu$ , and the deviation of the mutations,  $\sigma$ . Results for the case of a community with individuals whose probability distribution is characterized by the linear-quadratic case, eq. S36 are summarized in Figs. S5 and S6, whereas Fig. S7 corresponds to the quadratic-quartic case, eq. S37.

## S6.3 Co-evolutionary Model with K-body interactions

Are the previous results affected if a larger number of individuals is allowed to interact at each time step?

Parameter	Value
$N$	100
$M$	100
$\nu$	0.1
$\sigma$	0.1
$\sigma_{\beta_1}, \sigma_{\beta_2}$	$1\sigma, 0.1\sigma$
$T_i$	$10^4$
$T_f - T_i$	$10^5$
Init. Distribution	$N(-3, 0.25) \cdot N(-0.25, 0.05)$ $N(3, 0.25) \cdot N(0.25, 0.05)$ $U([-4, 4] \times [-0.8, 0.8])$
$R$	100 (10000 for transients)

**Supplementary Table S2:** Parameters of the simulation of the Co-evolutionary Model in Fig. 3 of the main text. See also Table S1.



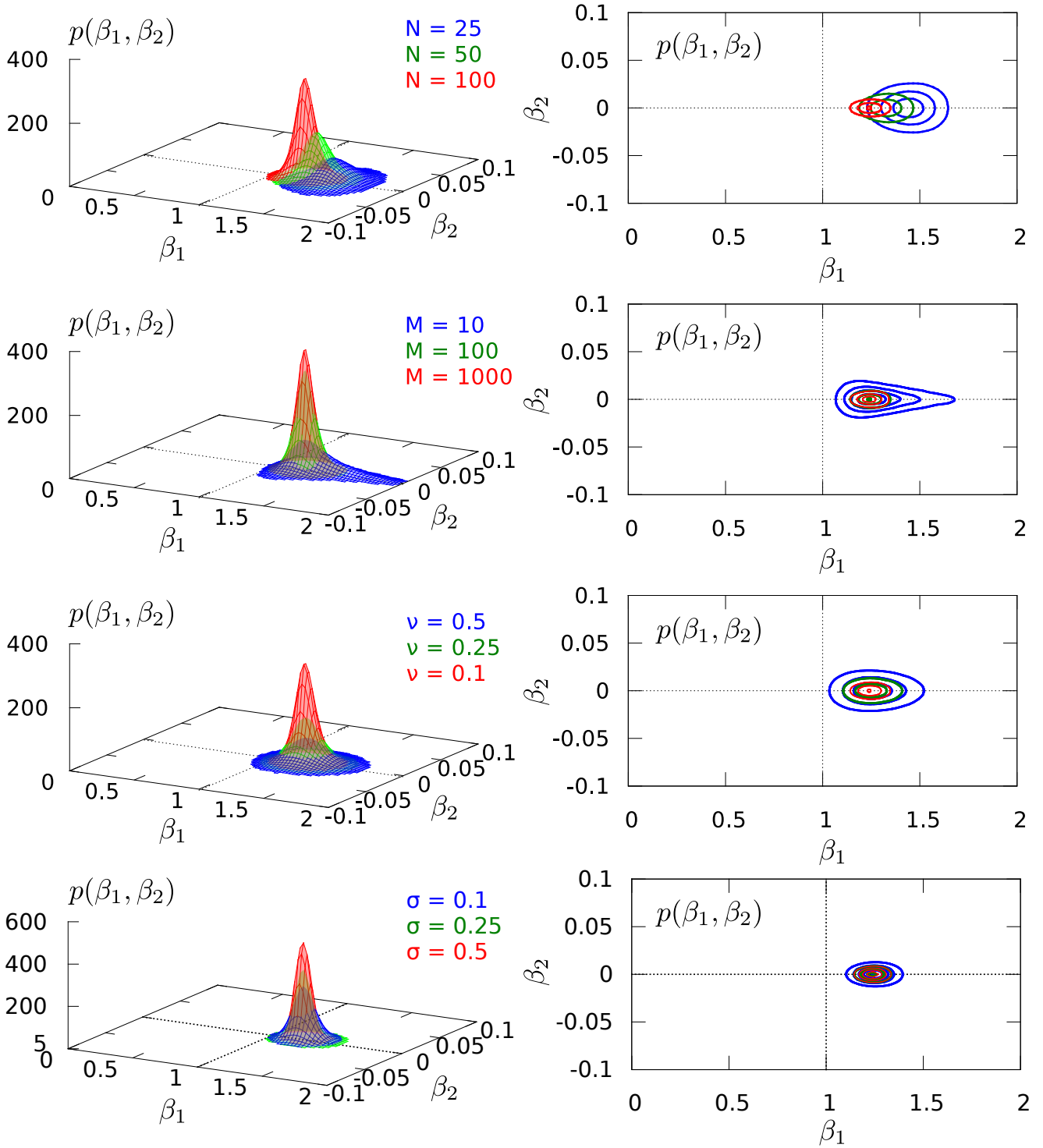
**Supplementary Figure S5:** *Time evolution in the Co-evolutionary Model* (in the linear-quadratic case, i.e. eq. S36). Plot of the mean values  $\langle \beta_{1,2} \rangle := \frac{1}{M} \sum_{k=1}^M \beta_{1,2}^k$  (top two panels) of the community, and parameter variance (bottom panel) for three different realizations started with different initial conditions  $p(\beta, t=0)$ : Gaussian distributions with two different averages and variances,  $N(-3, 0.25)N(-0.8, 0.05)$  for the red line and  $N(3, 0.25)N(0.8, 0.05)$  for the green one, and uniform distribution in the range  $[-4, 4] \times [-0.8, 0.8]$  for the blue one.

To answer this question, here we study a variant of the Co-evolutionary Model in which  $K$  individuals  $(i_1, \dots, i_K)$  are randomly picked at each time step, and they compete among themselves; the probability to die is proportional to its (normalized) average KL divergence to the remaining ones, i.e.

$$P_{kill}(i_k) = \frac{\sum_{l=1}^K D(\beta^{i_l} | \beta^{i_k})}{\sum_{m=1}^K \sum_{l=1}^K D(\beta^{i_l} | \beta^{i_m})},$$

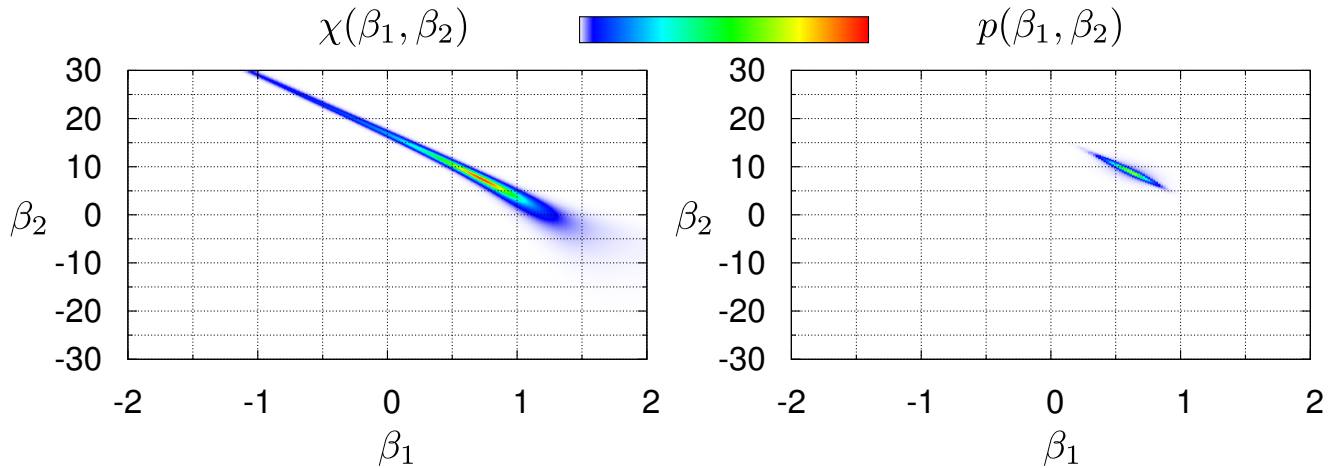
and then it is replaced by a copy of one of the remaining  $K - 1$  individuals (and mutations are introduced with probability  $\nu$ ).

We have implemented the simulation with parametrization of eq. S26. Results are summarized in Fig. S8

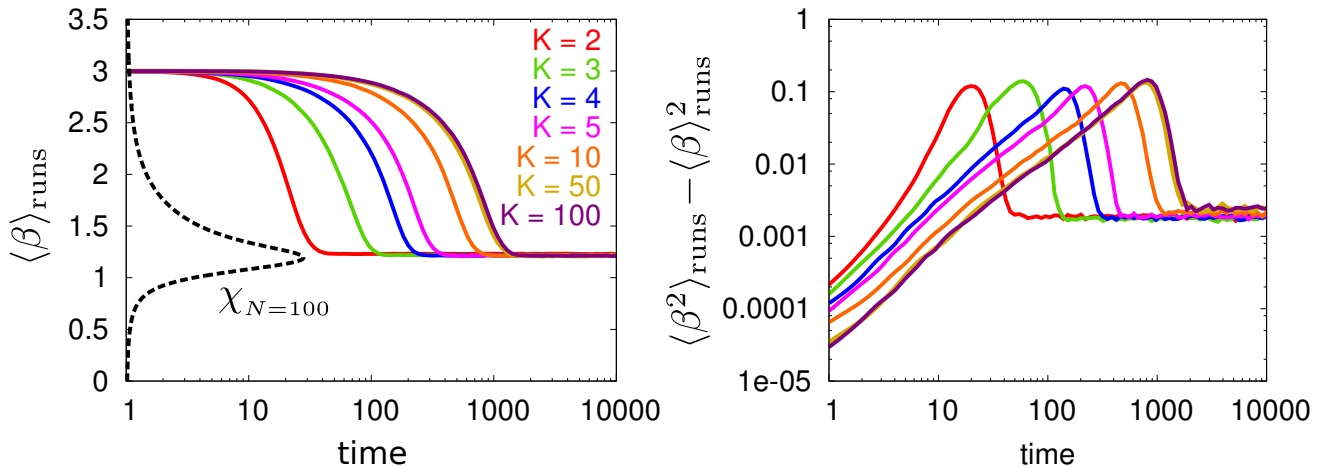


**Supplementary Figure S6:** *Dependence on parameters in the Co-evolutionary Model:* stationary distribution  $p(\beta_1, \beta_2)$  and its dependence on parameters (for the linear-quadratic case, eq. S36). Different colored lines in each plot correspond to different values of  $N$ , community sizes  $M$ , mutation probability  $\nu$  and mutation deviation  $\sigma$ . Parameters take the values of Table S2 (unless otherwise specified).

where we plot the mean value of the parameter over the entire community and  $10^3$  realizations of the same initial condition. It can be seen that the time to reach stationarity increases with  $K$ . When  $K$  increases, the drift which moves the system towards the criticality is lower. This is related to the fact that, by averaging over more and more individuals, the source effectively becomes more and more homogeneous.



**Supplementary Figure S7:** Stationary distribution  $p(\beta_1, \beta_2)$  in the Co-evolutionary Model, eq. S37: we compare the stationary distribution (right panel) with the determinant of susceptibility (left panel). Once again at stationarity, the individual parameters are at the peak of the determinant of the susceptibility. The community evolves toward the global maximum of the determinant of susceptibility at finite  $N$ . Parameters are set to  $N = 100$ ,  $M = 100$ ,  $\nu = 0.1$ ,  $\sigma_{\beta_1} = \sigma_{\beta_2} = 0.1$ .



**Supplementary Figure S8:** Time evolution in the Co-evolutionary Model with  $K$ -body interactions (with parametrization of eq. S26). Solid lines represent the time evolution of mean values  $\langle \beta \rangle := \int d\beta p(\beta, t)\beta$ . The relaxation to the stationary state depends on the effective number of individuals  $K$  with which each single agent interacts. Higher the  $K$ , the higher is the relaxation time. The community evolves very close to the maximum of the generalized susceptibility –in dashed line, coinciding with the specific heat in this case–. The initial condition is  $\beta = 3$  for all of the individuals and parameters are  $N = 100$ ,  $M = 100$ ,  $\nu = 1$  and  $\sigma = 0.1$ .

## S6.4 Co-evolutionary Model with complex distributions

We now scrutinize a different variant of the model in which the internal probability distribution of each individual/agent is not a “mean-field” one, in the sense that every  $s_i$  variable is coupled to all others, but instead, possible interactions are encoded in a network, such that each  $s_i$  interacts only with other  $s_j$  directly connected to it, i.e. for which the *adjacency matrix*, element  $a_{ij} \neq 0$ .

The evolutionary dynamics is as above, with the only difference that now the structure of the probability characterizing each individual is as follows:

- Given  $N$  spin variables, we generate a fixed adjacency matrix of interactions  $\hat{a}$ . The probability to find a certain configuration  $\mathbf{s}$  in the  $k$ -th individual is  $P_{\text{map}}^{\hat{a}}(\mathbf{s}|\beta^k) \propto \exp\{-H_{\text{map}}^{\hat{a}}(\mathbf{s}|\beta^k)\}$  with

$$H_{\text{map}}^{\hat{a}}(\mathbf{s}|\beta^k) = -\beta^k \frac{1}{N} \sum_{i,j>i} a_{ij} s_i s_j. \quad (\text{S38})$$

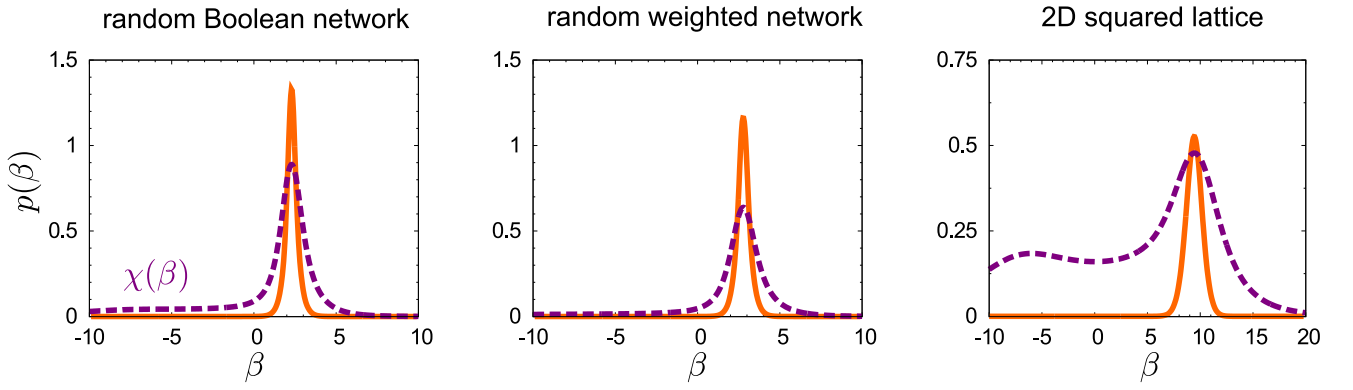
- The system is iterated as in the Co-evolutionary Model, leaving  $\hat{a}$  fixed in time and identical for all individuals.

As the structure of  $\hat{a}$  is an arbitrary one, the calculation of the distances between distributions needs to be explicitly computed by summing over the  $2^N$  possible states (which severely limits the maximum size in computer simulations;  $N \sim 20$ ).

Results for the stationary distribution of parameters  $p(\beta)$  and different types of network architectures, together with the corresponding curves of generalized susceptibilities computed as

$$\chi^{\hat{a}}(\beta) = \left\langle \left( \frac{1}{N} \sum_{i,j>i}^N a_{ij} s_i s_j \right)^2 \right\rangle_{P^{\hat{a}}(\mathbf{s}|\beta)} - \left\langle \frac{1}{N} \sum_{i,j>i}^N a_{ij} s_i s_j \right\rangle_{P^{\hat{a}}(\mathbf{s}|\beta)}^2 \quad (\text{S39})$$

are shown in Fig. S9. In all cases, the main result of this paper holds: the resulting map distributions peak around the critical point.



**Supplementary Figure S9:** Stationary parameter distributions for three different network structures  $\hat{a}$  of  $N$  nodes. Three cases are studied: **(left) Random Boolean network:** connections are not weighted, i.e.  $a_{ij} = a_{ji} = \{0, 1\}$ , with mean connectivity  $N/2$ , **(centre) Random weighted network:** in this case,  $a_{ij} = a_{ji} = \eta$ , where  $\eta$  is a random number between 0 and 1 **(right) Regular 2D lattice** with periodic bounding conditions. In all cases, parameters have been set to  $\nu = 0.1$ ,  $\sigma = 0.5$ ,  $M = 100$ . In the first two examples,  $N = 20$ , while  $N = 25$  for last one. In dashed line, the generalized susceptibility has been plotted and re-scaled for visual comparison.

## S7 Supplementary Videos

### Video 1: Simulation of the Evolutionary model leading to criticality in complex environments

*This video is available for download at [wdb.ugr.es/~hidalgoj/files/pmc/video1.avi](http://wdb.ugr.es/~hidalgoj/files/pmc/video1.avi)*

A community of agents or cognitive systems in different environments evolve according to a genetic algorithm. Every agent is represented with a black dot on the vertical axis. At each time step, different sources are generated from the colored region, every one characterized by a parameter  $\beta$ . The agents construct an internal map of the sources, represented in their own internal parameter  $\beta$ . Individuals with better representations have more chances to reproduce, and the offspring inherits the parameter  $\beta$  from their parents with a small mutation. We can see that, when the source pools are heterogeneous, as occurs for the left and right panels, the community evolves near the maximum of the Fisher Information, or, in other words, the critical point. However, when the sources are very specific, the agents do not become critical, as occur for the central panels.

### Video 2: Simulation of the Co-Evolutionary model leading self-consistently to criticality

*This video is available for download at [wdb.ugr.es/~hidalgoj/files/pmc/video2.avi](http://wdb.ugr.es/~hidalgoj/files/pmc/video2.avi)*

A community of agents or cognitive systems co-evolve according to a genetic algorithm. Different colors represent different initial conditions and so individuals of different colors do not interact with each other. Each agent constructs a map of the rest of the community, represented with a dot in the two parameter space ( $\beta_1$  and  $\beta_2$ ). As in Video 1, individuals with better representations reproduce more probably, and the offspring inherits the parameters from their parents with small mutations. The simulation shows how, independently of the initial condition, the individuals self-tune to the maximum of the Fisher information or critical point.

### Video 3: Simulation of the Co-Evolutionary model for small systems

*This video is available for download at [wdb.ugr.es/~hidalgoj/files/pmc/video3.avi](http://wdb.ugr.es/~hidalgoj/files/pmc/video3.avi)*

As in Video 2, a community of agents or cognitive systems co-evolve to understand each other. Each agent constructs a map of the environment, represented with a dot in the two parameter space ( $\beta_1$  and  $\beta_2$ ). The information is encoded in strings of  $N$  binary variables. Every agent has  $N = 10$  in the upper panel and 100 in the lower one. The Fisher Information for the two parameters map is plotted in the background. We can see how, after iterating the genetic algorithm, the agents localize at the maximum of the Fisher Information. When  $N$  increases, the peak approaches the critical point.

## References

- [1] Stanley, H. E. *Introduction to phase transitions and critical phenomena* (Oxford University Press, 1987).
- [2] Binney, J., Dowrick, N., Fisher, A. & Newman, M. *The Theory of Critical Phenomena* (Oxford University Press, Oxford, 1993).
- [3] Langton, C. Computation at the edge of chaos: Phase transitions and emergent computation. *Physica D: Nonlinear Phenomena* **42**, 12–37 (1990).
- [4] Bertschinger, N. & Natschläger, T. Real-time computation at the edge of chaos in recurrent neural networks. *Neural Computation* **16**, 1413–1436 (2004).
- [5] Sporns, O., Chialvo, D., Kaiser, M., Hilgetag, C. *et al.* Organization, development and function of complex brain networks. *Trends in cognitive sciences* **8**, 418–425 (2004).
- [6] Chialvo, D. R. Emergent complex neural dynamics. *Nature Physics* **6**, 744–750 (2010).

- [7] Haimovici, A., Tagliazucchi, E., Balenzuela, P. & Chialvo, D. R. Brain organization into resting state networks emerges at criticality on a model of the human connectome. *Phys. Rev. Lett* **110**, 178101 (2013).
- [8] Legenstein, R. & Maass, W. Edge of chaos and prediction of computational performance for neural circuit models. *Neural Networks* **20**, 323–334 (2007).
- [9] Beggs, J. M. The criticality hypothesis: How local cortical networks might optimize information processing. *Phil. Trans. R. Soc. A* **366**, 329–343 (2008).
- [10] Kinouchi, O. & Copelli, M. Optimal dynamical range of excitable networks at criticality. *Nature Physics* **2**, 348–351 (2006).
- [11] Beggs, J. & Plenz, D. Neuronal avalanches in neocortical circuits. *The Journal of neuroscience* **23**, 11167–11177 (2003).
- [12] Proekt, A., Banavar, J., Maritan, A. & Pfaff, D. Scale invariance in the dynamics of spontaneous behavior. *Proceedings of the National Academy of Sciences* **109**, 10564–10569 (2012).
- [13] Nykter, M. *et al.* Gene expression dynamics in the macrophage exhibit criticality. *Proceedings of the National Academy of Sciences* **105**, 1897–1900 (2008).
- [14] Furusawa, C. & Kaneko, K. Adaptation to optimal cell growth through self-organized criticality. *Phys Rev Lett* **108**, 208103 (2012).
- [15] Chen, X., Dong, X., Be'er, A., Swinney, H. & Zhang, H. Scale-invariant correlations in dynamic bacterial clusters. *Physical Review Letters* **108**, 148101 (2012).
- [16] Bialek, W. *et al.* Statistical mechanics for natural flocks of birds. *Proceedings of the National Academy of Sciences* **109**, 4786–4791 (2012).
- [17] Mora, T. & Bialek, W. Are biological systems poised at criticality? *Journal of Statistical Physics* **144**, 268–302 (2011).
- [18] Kullback, S. & Leibler, R. A. On information and sufficiency. *The Annals of Mathematical Statistics* **22**, 79–86 (1951).
- [19] Cover, T. M. & Thomas, J. *Elements of Information Theory* (Wiley, 1991).
- [20] Sanov, I. N. *On the probability of large deviations of random variables*, vol. 42 (1957).
- [21] Mezard, M. & Montanari, A. *Information, physics, and computation* (OUP Oxford, 2009).
- [22] Ackley, D. H., Hinton, G. E. & Sejnowski, T. J. A learning algorithm for boltzmann machines. *Cognitive science* **9**, 147–169 (1985).
- [23] Goldberg, D. E. *Genetic Algorithms in Search, Optimization, and Machine Learning* (Addison-Wesley Professional, 1989).
- [24] Mitchell, M. *An Introduction to Genetic Algorithms (Complex Adaptive Systems)* (MIT Press, 1998).